Spontaneous currents in Josephson junctions between unconventional superconductors and *d*-wave qubits (Review)

Yu. A. Kolesnichenko* and A. N. Omelyanchouk

B. Verkin Institute for Low Temperature Physics and Engineering of the National Academy of Sciences of Ukraine, 47 Lenin Ave., Kharkov 61103, Ukraine

A. M. Zagoskin

*D-Wave Systems Inc., 320-1985 West Broadway, Vancouver, B.C., V6J 4Y3, Canada;
The University of British Columbia, 6224, Agricultural Rd., Vancouver, B.C., V6T 1Z1, Canada*

The modern physics of superconductivity can be called the physics of unconventional superconductivity. The discovery of the *d*-wave symmetry of the order parameter in high-temperature superconductors and the triplet superconductivity in compound Sr_2RuO_4 has caused a huge stream of theoretical and experimental investigations of unconventional superconductors. In this review we discuss some novel aspects of the Josephson effect which are related to the symmetry of the order parameter. The most intriguing of them is spontaneous current generation in an unconventional weak link. The example of a Josephson junction in the form of a grain boundary between two disorientated *d*-wave or *f*-wave superconductors is considered in detail. Josephson current–phase relations and the phase dependences of the spontaneous current that flows along the interface are analyzed. The spontaneous current and spontaneous phase difference are manifestations of the time-reversal symmetry ($\mathcal{T}$) breaking states in the system. We analyzed the region of appearance of $\mathcal{T}$-breaking states as function of temperature and mismatch angle. A review of the basics of superconducting qubits with emphasis on specific properties of *d*-wave qubits is given. Recent results in the problem of decoherence in *d*-wave qubits, which is the major concern for any qubit realization, are presented. © *2004 American Institute of Physics.* [DOI: 10.1063/1.1789112]

1. INTRODUCTION

The modern physics of superconductivity can be called the physics of unconventional superconductivity. It should be noted that right after the famous paper[1] of Bardeen, Cooper, and Schriffer (BCS) it became clear that (conventional) *s*-wave singlet pairing is not the only possibility,[2,3] and more-complex superconducting (superfluid) states may be realized, with nonzero orbital and spin momenta of the Cooper pairs. Because of the success of the BCS theory in describing properties of the known metallic superconductors, theoretical research on unconventional superconductivity was of purely academic interest and did not attract much attention. Interest in unconventional pairing symmetry has increased after the discovery of superfluidity in ^{3}He, with triplet spin symmetry and multiple superfluid phases.[4,5] Low-temperature experiments on complex compounds led to the discovery of unconventional superconductivity in heavy-fermion systems.[6] The heavy-fermion metal UPt_3, like ^{3}He, has a complex superconducting phase diagram, which shows the existence of several superconducting phases, while a weak temperature dependence of the paramagnetic susceptibility indicates triplet pairing. Another triplet superconductor is the recently discovered compound Sr_2RuO_4.

The real boom in investigations of unconventional superconductivity started after the discovery by Bednorz and Müller[7] of high-temperature (high-T_c) superconductivity in cuprates, because of its fundamental importance for both ba-sic science and practical applications. Numerous experiments show that high-T_c cuprates are singlet superconductors with nontrivial orbital symmetry of the order parameter (a so-called *d*-wave state, with the orbital moment of pairs $l=2$).

The Josephson effect[8] is extremely sensitive to the dependence of the complex order parameter on the momentum direction on the Fermi surface. Thus the investigation of this effect in unconventional superconductors enables one to distinguish among different candidates for the symmetry of the superconducting state. This has stimulated numerous theoretical and experimental studies of unconventional Josephson weak links. One of the possibilities for forming a Josephson junction is to create a point contact between two massive superconductors. A microscopic theory of the stationary Josephson effect in ballistic point contacts between conventional superconductors was developed in Ref. 9. Later this theory was generalized for a pinhole model in ^{3}He,[10,11] for point contacts between *d*-wave high-T_c superconductors,[12–14] and for triplet superconductors.[15] A detailed theory of the Josephson properties of grain-boundary *d*-wave junctions was developed in Ref. 16. In those papers it was shown that the current–phase relations for the Josephson current in unconventional weak links are quite different from those of conventional superconductors. One of the most striking manifestations of a unconventional order-parameter symmetry is the appearance, together with the Josephson current, of a spontaneous current flowing along the contact

interface. The spontaneous current arises due to the breaking of the time-reversal symmetry ($\mathcal{T}$) in the system. Such a situation takes a place, for example, in a junction between two *d*-wave superconductors with different crystallographic orientations. The *d*-wave order parameter itself doesn't break the $\mathcal{T}$ symmetry. But the mixture of two differently oriented order parameters (proximity effect) forms a $\mathcal{T}$-breaking state near the interface.[17] Such spontaneous supercurrent j_{spon} (and corresponding spontaneous phase difference) exists even if the net Josephson current equals zero. The state of the junction with the spontaneous current is twofold degenerate, and in fact, two values $\pm j_{\mathrm{spon}}$ appear. An interesting possibility arises then to use these macroscopic quantum states for the design of *d*-wave quantum bits (qubits).

This review consists of three parts. In Sec. 2 the general features of unconventional superconductivity are presented. The different types of order parameters are described. We briefly outline the essence of $\mathcal{T}$-symmetry breaking in unconventional superconductors and experimental tests for order-parameter symmetry. In Sec. 3 (and Appendix II) the theory of coherent current states in Josephson junctions between *d*-wave superconductors and between triplet superconductors is considered. The current–phase relations for the Josephson and spontaneous currents, as well as the bistable states, are analyzed. Section 4 is devoted to Josephson phase qubits based on *d*-wave superconductors. It contains a review of the basics of superconducting qubits with emphasis on specific properties of *d*-wave qubits. Recent results in the problem of decoherence in *d*-wave qubits, which is the major concern for any qubit realization, are presented.

2. UNCONVENTIONAL SUPERCONDUCTIVITY

2.1. Order-parameter in unconventional superconductors. *s*-wave, *d*-wave, *p*-wave ... pairing

The classification and description of unconventional superconducting states can be found, for example, in the book[18] and review articles.[19–23] In our review we do not aim to discuss this problem in detail. We present only general information on the unconventional superconductors and their most likely model descriptions.

It is well known[1] that a Cooper pair has zero orbital momentum, and its spin can be either $S=0$ (singlet state) or $S=1$ (triplet state). It follows from the Pauli exclusion principle that the matrix order parameter of the superconductor $\Delta_{\alpha\beta}(\mathbf{k})$ (α,β are spin indices) changes sign under permutation of particles in the Cooper pair: $\Delta_{\alpha\beta}(\mathbf{k})=-\Delta_{\beta\alpha}(-\mathbf{k})$. Hence, the even parity state is a singlet state with zero spin moment, $S=0$:

$$\hat{\Delta}^{(\mathrm{singlet})}(\mathbf{k})=g(\mathbf{k})i\hat{\sigma}_y;$$

$$g(\mathbf{k})=g(-\mathbf{k}). \tag{1}$$

The odd parity state is a triplet state with $S=1$, which is in general a linear superposition of three substates with different spin projection $S_z=-1,0,1$:

$$\hat{\Delta}^{(\mathrm{triplet})}(\mathbf{k})=(\mathbf{d}(\mathbf{k})\sigma)\hat{\sigma}_y;$$

$$\mathbf{d}(-\mathbf{k})=-\mathbf{d}(\mathbf{k}). \tag{2}$$

Here the $\hat{\sigma}_i$ are Pauli matrices ($i=x,y,z$); $\mathbf{d}(\mathbf{k})$ and $\sigma=(\hat{\sigma}_x,\hat{\sigma}_y,\hat{\sigma}_z)$ are vectors in the spin space. The components of the vector $\mathbf{d}(\mathbf{k})$ are related with the amplitudes $g_{S_z}(k)$ of states with different spin projections $S_z=(-1,0,1)$ on the quantization axis:

$$g_1=-d_x+id_y;\quad g_0=d_z;\quad g_{-1}=d_x+id_y. \tag{3}$$

The functions $g(\mathbf{k})$ and $\mathbf{d}(\mathbf{k})$ are frequently referred to as an order parameter of the superconductor. For the isotropic model $g(\mathbf{k})=\mathrm{const}$ the paring state is singlet. In a triplet superconductor the order parameter $\mathbf{d}(\mathbf{k})$ is a vector (some authors call it the gap vector) in the spin space and in any case it depends on the direction on the Fermi surface. This vector defines the axis along which the Cooper pairs have zero spin projection.

The angular dependence of the order parameter is defined by the symmetry group $\mathcal{G}$ of the normal state and the symmetry of the electron interaction potential, which can break the symmetry $\mathcal{G}$. In a model of an isotropic conductor the quantum states of the electron pair can be described in terms of an orbital momentum l and its z projection m. The singlet (triplet) superconducting state is the state with an even (odd) orbital momentum l of Cooper pairs. The respective states are labeled by letters $s,p,d,\ldots$ (similar to the labeling of electron orbital states in atom) and are called *s*-wave, *p*-wave, *d*-wave, ... states. In the general case the superconducting state may be a mixture of states with different orbital momenta l.

The spherically symmetrical superconducting state, which now is frequently called the conventional one, corresponds to *s*-wave singlet pairing $l=m=S=0$. In this case of isotropic interaction, the order parameter is a single complex function $g=\mathrm{const}$. Fortunately, this simple model satisfactorily describes the superconductivity in conventional metals, where the electron–phonon interactions leads to spin-singlet pairing with *s*-wave symmetry. The simplest triplet superconducting state is the state with *p*-wave pairing and orbital momentum of a Cooper pair $l=1$. In the case of *p*-wave pairing different superconducting phases with different $m=-1,0,1$ are possible. A Cooper pair in a *p*-wave superconductor has internal structure, because for $l=1$ it is intrinsically anisotropic. The next singlet *d*-wave state has the orbital momentum of Cooper pairs $l=2$.

In unconventional superconducting states the Cooper pairs may have a nonzero expectation value of the orbital $\mathbf{L}$ or (and) spin $\mathbf{S}$ momentum of a pair. States with $\mathbf{S}\neq0$ ($\mathbf{S}=0$) are usually called nonunitary (unitary) triplet states.

The gap $\Delta(\mathbf{k})$

$$\Delta^2(\mathbf{k})=\tfrac{1}{2}\mathrm{Tr}\hat{\Delta}^\dagger(\mathbf{k})\hat{\Delta}(\mathbf{k}) \tag{4}$$

in the energy spectrum of elementary excitations is given by the relations

$$\Delta^{(\mathrm{singlet})}(\mathbf{k})=|g(\mathbf{k})|; \tag{5}$$

$$\Delta^{(\mathrm{triplet})}(\mathbf{k})=\sqrt{[|\mathbf{d}(\mathbf{k})|^2\pm|\mathbf{d}(\mathbf{k})\times\mathbf{d}^*(\mathbf{k})|]}. \tag{6}$$

In unconventional superconductors the gap can be equal to zero for some directions on the Fermi surface, and for nonunitary states ($\mathbf{S}\neq0$, so-called magnetic superconductors) the energy spectrum has two branches.

In the absence of magnetic field the transition to a superconducting state is a second-order phase transition. According to the Landau theory[24] of second-order phase transitions, the order parameter of such a state must transform according to one of the irreducible representations of the point symmetry group $\mathcal{G}$ of the normal phase, i.e., the symmetry group of the superconducting state is a subgroup of the symmetry group of the normal state. The symmetry group $\mathcal{G}$ of the normal state contains the symmetry operations $G_{\text{spin-orbit}}$ in spin and orbital (coordinate) spaces, the operation of time reversal $\mathcal{T}$, and the gauge transformation $U(1)$:

$$\mathcal{G} = U(1) \times \mathcal{T} \times G_{\text{spin-orbit}}.$$

The transition to a superconducting state breaks the gauge symmetry $U(1)$, and states with different phases of the order parameter become distinguishable. The conventional superconducting state is described by the symmetry group $H = \mathcal{T} \times G_{\text{spin-orbit}}$. If another point symmetry property of the superconducting state is broken, such a superconductor is termed an unconventional one. The order parameter of different superconducting states can be expanded on basis functions of different irreducible representations of the point symmetry group G. For non-one-dimensional representations the order parameter is a sum of a few complex functions with different phases, and such an order parameter is called a multicomponent one.

In real crystalline superconductors there is no classification of Cooper pairing by angular momentum (*s*-wave, *p*-wave, *d*-wave, *f*-wave pairing, etc.). However, these terms are often used for unconventional superconductors, meaning that the point symmetry of the order parameter is the same as that for the corresponding representation of the $SO(3)$ symmetry group of an isotropic conductor. In this terminology conventional superconductors can be referred to as *s*-wave. If the symmetry of $\hat{\Delta}$ cannot be formally related to any irreducible representation of the $SO(3)$ group, these states are usually referred to as hybrid states.

2.2. Pairing symmetry in cuprate and triplet superconductors

Cuprate superconductors. All cuprate high-temperature superconductors ($La_{2-x}Sr_xCuO_4$, $Tl_2Ba_2CaCu_2O_8$, $HgBa_2CaCu_2O_6$, $YBa_2Cu_3O_7$, $YBa_2Cu_3O_{7-\delta}$, $Bi_2Sr_2CaCu_2O_8$ and others) have a layered structure with the common structural ingredient—the CuO_2 planes. In some approximation these compounds may be considered as quasi-two-dimensional metals having a cylindrical Fermi surface. It is generally agreed that superconductivity in cuprates basically originates from the CuO_2 layers. Knight shift measurements[25] below T_c indicate that in the cuprate superconductors pairs form spin singlets, and therefore even-parity orbital states.

The data of numerous experiments (see, for example, the review article[19]), in which the different properties of cuprate superconductors had been investigated, and the absence of multiple superconducting phases attests that the superconducting state in this compounds is most probably described by a one-component nontrivial order parameter of the form

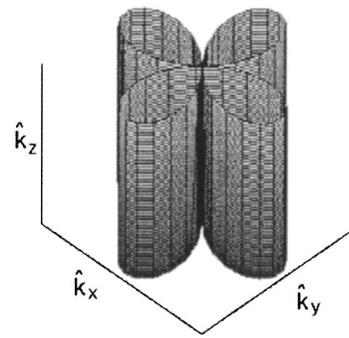$$g(\mathbf{k}) = \Delta(T)(\hat{k}_x^2 - \hat{k}_y^2), \qquad (7)$$

FIG. 1. The modulus of the order parameter $|g(\mathbf{k})|$ (7) in momentum space for a *d*-wave superconductor.

where $\Delta(T)$ is a real scalar function, which depends only on the temperature T, and $\hat{\mathbf{k}} = (\hat{k}_x, \hat{k}_y)$. This type of pairing is a two-dimensional analog of the singlet superconducting state with $l = 2$ in an isotropic metal and usually is called "*d*-wave" (or $d_{x^2-y^2}$) pairing. The excitation gap $|g(\mathbf{k})|$ has four line nodes on the Fermi surface at $\varphi_n = (\pi/4)(2n+1)$, $n = 0,1,2,3$ (Fig. 1), and the order parameter $g(\mathbf{k})$ changes sign in momentum space.

Triplet superconductivity, an analog of triplet superfluidity in ^{3}He, was first discovered in the heavy-fermion compound UPt$_3$ more than ten years ago.[26,27] Other triplet superconductors have been found recently: Sr$_2$RuO$_4$ (Refs. 28, 29) and (TMTSF)$_2$PF$_6$ (Ref. 30). In these compounds, the triplet pairing can be reliably determined, e.g., by Knight shift experiments.[31–33] It is, however, much harder to identify the symmetry of the order parameter. Apparently, in crystalline triplet superconductors the order parameter depends on the direction in momentum space, $\hat{\mathbf{k}}$, in a more complicated way than the well-known *p*-wave behavior of the superfluid phases of ^{3}He. While numerous experimental and theoretical works have investigated various thermodynamic and transport properties of UPt$_3$ and Sr$_2$RuO$_4$, the precise order-parameter symmetry is still to be determined (see, e.g., Refs. 34–37 and references therein). Symmetry considerations allow considerable freedom in the choice of irreducible representation and its basis. Therefore numerous authors (see, for example, Refs. 34–40) consider different models (so-called scenarios) of superconductivity in UPt$_3$ and Sr$_2$RuO$_4$, based on possible representations of crystallographic point groups. A conclusion as to the symmetry of the order parameter can be reached only after a comparison of the theoretical results with experimental data.

Pairing symmetry in Sr$_2$RuO$_4$. In experiment, Sr$_2$RuO$_4$ shows clear signs of triplet superconductivity below the critical temperature $T_c = 1.5$ K. Investigation of the specific heat,[41] penetration depth,[42] thermal conductivity,[43] and ultrasound absorption[44] shows a power-law temperature dependence, which is evidence of line nodes in the energy gap in the spectrum of excitations. The combination of these results with the Knight shift experiment[32] led to the conclusion that Sr$_2$RuO$_4$ is an unconventional superconductor with spin-triplet pairing. A layered perovskite material, Sr$_2$RuO$_4$ has a quasi-two-dimensional Fermi surface.[45]

The first candidate for the superconducting state in Sr$_2$RuO$_4$ was the "*p*-wave" model[45–47]

$$\mathbf{d}(\mathbf{k}) = \Delta\hat{z}(\hat{k}_x \pm i\hat{k}_y). \tag{8}$$

The order parameter of the form (8) is a two-dimensional analog ($\hat{\mathbf{k}} = (\hat{k}_x, \hat{k}_y)$) of the order parameter in the A phase of ^{3}He. The **d** vector pointing along the z direction implies that the spin part of the Cooper pair wave function is the spin-triplet state with $S_z = 0$, i.e., in-plane equal-spin pairing (the z direction is along the c axis of Sr_2RuO_4). In a system with cylindrical symmetry the orbital part of the pair wave function is a state with finite angular momentum along the z axis, $L_z = \pm 1$.

However, the model (8) does not describe the whole corpus of the experimental data. Recently[36,37] it was shown that the pairing state in Sr_2RuO_4 most likely has lines of nodes, and some others models of the order parameter have been proposed:[36,37]

$$\mathbf{d}(\mathbf{k}) = \Delta\hat{z}\hat{k}_x\hat{k}_y(\hat{k}_x \pm \hat{k}_y). \tag{9}$$

$$\mathbf{d}(\mathbf{k}) = \Delta\hat{z}(\hat{k}_x^2 - \hat{k}_y^2)(\hat{k}_x \pm i\hat{k}_y). \tag{10}$$

In unitary states (8)–(10) the Cooper pairs have $L = \pm 1$ and $S = 0$.

Theoretical studies of specific heat, thermal conductivity, and ultrasound absorption for different models of triplet superconductivity show considerable quantitative differences between calculated dependences for "p-wave" and "f-wave" models.[34–36,40]

Heavy fermion superconductor UPt_3. One of the best-investigated heavy fermion superconductors is the heavy-fermion compound UPt_3 (Refs. 34 and 35). The weak temperature dependence of the Knight shift,[31] multiple superconducting phases,[26] unusual temperature dependence of the heat capacity,[48] thermal conductivity,[49,50] and sound absorption[51] in UPt_3 show that it is a triplet unconventional superconductor with a multicomponent order parameter.

The heavy-fermion superconductor UPt_3 belongs to the hexagonal crystallographic point group D_{6h}. The models which have been successful in explaining the properties of the superconducting phases in UPt_3 is based on the odd-parity two-dimensional representation E_{2u}. These models describe the hexagonal analog of spin-triplet f-wave pairing.

One of the models corresponds to the strong spin–orbital coupling with vector **d** locked along the lattice **c** axis ($\mathbf{c} \| \hat{z}$).[34,35] For this model $\mathbf{d} = \hat{z}[\eta_1 Y_1 \pm \eta_2 Y_2]$, where $Y_1 = k_z(k_x^2 - k_y^2)$ and $Y_2 = 2k_x k_y k_z$ are the basis functions of the representation. For the high-temperature polar phase ($\eta_1 = 1, \eta_2 = 0$)

$$\mathbf{d}(\mathbf{k}) = \Delta\hat{z}\hat{k}_z(\hat{k}_x^2 - \hat{k}_y^2), \tag{11}$$

and for the low-temperature axial phase ($\eta_1 = 1, \eta_2 = i$)

$$\mathbf{d}(\mathbf{k}) = \Delta\hat{z}\hat{k}_z(\hat{k}_x \pm \hat{k}_y)^2, \tag{12}$$

where $\hat{\mathbf{k}} = (\hat{k}_x, \hat{k}_y, \hat{k}_z)$.

Both are unitary states. The state (11) has zero expectation value of orbital momentum, while in the state (12) $\langle L \rangle = \pm 2$. For the polar phase (11) the gap in the energy spectrum of excitations $|\mathbf{d}(\mathbf{k})|$ has an equatorial nodal line at $\theta = \pi/2$ and longitudinal nodal lines at $\varphi_n = (\pi/4)(2n+1)$, $n = 0,2,3,4$ (Fig. 2). In the axial state (12) the longitudinal
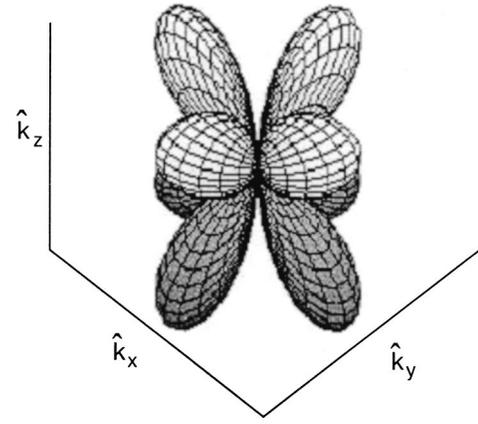
FIG. 2. The modulus of the order parameter $|\mathbf{d}(\mathbf{k})|$ (11) in momentum space for the polar phase in an f-wave superconductor.

line nodes are closed and there is a pair of point nodes $\theta = 0, \pi$ (Fig. 3).

Other orbital state candidates, which assume weak effective spin–orbital coupling in UPt_3, are the unitary planar state

$$\mathbf{d}(\mathbf{k}) = \Delta\hat{k}_z[\hat{x}(\hat{k}_x^2 - \hat{k}_y^2) + 2k_x k_y \hat{y}], \tag{13}$$

and the nonunitary bipolar state

$$\mathbf{d}(\mathbf{k}) = \Delta\hat{k}_z[\hat{x}(\hat{k}_x^2 - \hat{k}_y^2) + 2ik_x k_y \hat{y}]. \tag{14}$$

More models for the order parameter in UPt_3 are discussed in Refs. 21, 34 and 35. The models (8)–(10), (12), (14) are interesting in that they spontaneously break time-reversal symmetry ($\mathcal{T}$-breaking), which we discuss in the next Section.

2.3. Breaking of the time-reversal symmetry in unconventional superconductors. Spontaneous magnetic fields and currents

Time-reversal symmetry means that the Hamiltonian $\mathcal{H} = \mathcal{H}^*$, because if $\psi(\mathbf{r})$ is a solution of the Schrödinger equation, then $\psi^*(\mathbf{r})$ is also a solution of the same equation. The time-reversal operation $\mathcal{T}$ is equivalent to complex conjugation $\mathcal{T}\hat{\Psi} = \hat{\Psi}^*$. The simplest example, when both the time-
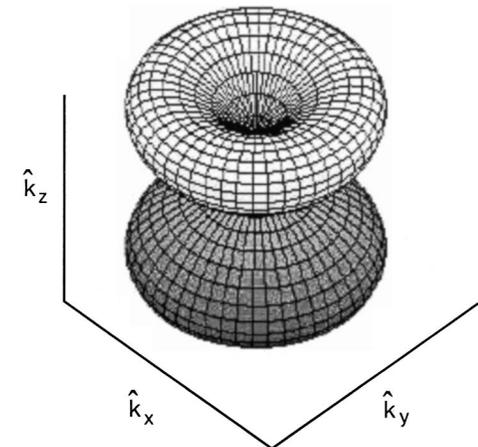
FIG. 3. The modulus of the order parameter $|\mathbf{d}(\mathbf{k})|$ (12) in momentum space for the axial phase in an f-wave superconductor.

reversal symmetry $\mathcal{T}$ and parity $\mathcal{P}$ are broken, is a charged particle in an external magnetic field **H**, where $\psi(\mathbf{r},\mathbf{H})$ and $\psi^*(\mathbf{r},-\mathbf{H})$ are solutions of the Schrödinger equation, while $\psi(\mathbf{r},-\mathbf{H})$ and $\psi^*(\mathbf{r},\mathbf{H})$ describe different degenerate states of the system. This fact is crucial for understanding of the appearance of nondissipative (persistent) currents in mesoscopic rings, that reflects the broken clockwise–counterclockwise symmetry of electron motion along the ring, caused by the external vector potential.

Unconventional superconductivity allows for a large variety of possible phases. In some of them $\mathcal{T}$ and $\mathcal{P}$ are violated; such superconductors are frequently called *chiral* ones. (The word "chiral," literally "handed," was first introduced into science by Lord Kelvin (William Thomson) in 1884.) The time reversal (that is, complex conjugation) of a one-component order parameter is equivalent to its multiplication by a phase factor and does not change the observables. Therefore only in unconventional superconductors with a multicomponent order parameter can the $\mathcal{T}$-symmetry be broken. In particular, all superconducting states possessing nonzero orbital or/and spin momenta are chiral ones.

If the $\mathcal{T}$-symmetry is broken, the superconducting phase is determined not only by the symmetry of the order parameter but also by the topology of the ground state. The latter is characterized by the integer-valued topological invariant N in momentum space.[52–58] Among the various implications of chirality, perhaps the most striking is the set of chiral quasiparticle states, localized at the surface. These chiral states carry spontaneous dissipation-free currents along the surface. They are gapless, in contrast to bulk quasiparticles of the superconductor.[55]

Volovik and Gor'kov[52] have classified chiral superconducting states into two categories, the so-called "ferromagnetic" and "antiferromagnetic" states. They are distinguished by the internal angular moment of the Cooper pairs. In the "ferromagnetic" state the Cooper pairs possess a finite orbital or (for nonunitary states) spin moment, while in the "antiferromagnetic" state they have no net moments.

In high-temperature superconductors with the order parameter (7) the time reversal $\mathcal{T}$-symmetry is preserved in the bulk. However, it has been shown theoretically (see the review[22] and references therein) that the pure $d_{x^2-y^2}$ pair state is not stable against the $\mathcal{T}$-breaking states, such as $d_{x^2-y^2}+id_{xy}$ or $d_{x^2-y^2}+is$, at surfaces and interfaces, near impurities, or below a certain characteristic temperature (d_{xy} or s means an admixture of the d-wave state with $g(\mathbf{k})\sim 2k_xk_y$ or the s-wave state with $g(\mathbf{k})=$const. It turns out that such states have larger condensation energy. The $d_{x^2-y^2}+id_{xy}$-wave state represents a ferromagnetic pairing state, while the $d_{x^2-y^2}+is$-wave state is antiferromagnetic.

Among the heavy-fermion superconductors there are two well-known systems which have $\mathcal{T}$-violating bulk superconducting phases: UPt$_3$ and U$_{1-x}$Th$_x$Be$_{13}$ ($0.017<x<0.45$). These materials show double superconducting transitions on decreasing temperature, and $\mathcal{T}$-violation is associated with the second of them. The proposed models (12) and (14) of the order parameter in UPt$_3$ correspond to the $\mathcal{T}$-violating states. A more recent candidate for $\mathcal{T}$-violating superconductivity is Sr$_2$RuO$_4$. The "p-wave" and "f-wave" unitary models (8)–(10) describe the $\mathcal{T}$-violating bulk superconduct-

ing phases with finite orbital moments of the Cooper pairs.

$\mathcal{T}$-breaking leads to interesting macroscopic physics in a superconductor. Local currents generating orbital angular momenta flow in the bulk. In general, superconductivity and magnetism are antagonistic phenomena, but in this case, the superconducting state generates its own magnetism. The Meissner–Ochsenfeld effect, however, prevents uniform magnetization inside the superconductor, and magnetism is restricted to areas of inhomogeneities—that is, around impurities and domain walls or at interfaces and surfaces. In these regions, spontaneous supercurrents flow. The surface current generates a spontaneous magnetic moment.[59,60] In triplet superconductors all nonunitary models break time-reversal symmetry. For these states Cooper pairs have finite spins, while the magnetization in the bulk is negligible. It was demonstrated that chiral superconductors could show quantum Hall-like effects even in the absence of an external magnetic field:[61] a transverse potential difference would appear in response to the supercurrent.

2.4. Tests for order parameter in unconventional superconductors

The simplest way to test the unconventional superconducting state is to investigate the effect of impurity scattering on kinetic and thermodynamic characteristics. For s-wave superconductors, nonmagnetic impurities have no effects on T_c (Anderson's theorem). In superconductors with unconventional pairing the nonmagnetic impurities induce pair-breaking and suppress superconductivity. Increasing impurity concentration leads to the isotropization of the order parameter. In the state with broken spatial symmetry the only way to achieve it is make the order parameter to zero over entire Fermi surface. This happens if $\Delta_0\tau\sim 1$, where Δ_0 is of the order of the average gap magnitude in the absence of impurities at $T=0$, and τ is the quasiparticles' mean free time.[62–64]

The Knight shift $\delta\omega$ of the nuclear magnetic resonance (NMR) frequency (for details, see Ref. 65) is the most suitable instrument for determining the spin structure of the superconducting state. Because it results from electron interaction with nuclear magnetic moments, $\delta\omega$ is proportional to the Pauli paramagnetic susceptibility χ of normal electrons, the temperature dependence of $\delta\omega(T)$ depends strongly on whether the pairing is singlet or triplet. In singlet superconductors the Cooper pair spin $S=0$, and the density of normal electrons goes to zero at $T\to 0$. Therefore $\delta\omega\to 0$ as well. In triplet superconductors both Cooper pairs and excitations contribute to the susceptibility χ, which changes little with decreasing temperature.

The presence of point and line nodes of the order parameter in unconventional superconductors may be determined from the temperature dependence of thermodynamic quantities and transport coefficients. In fully gapped ($\Delta=$const) s-wave superconductors they display thermally activated behavior ($\sim\exp(-\Delta/T)$). In a superconductor with nodes in the gap of the elementary excitation spectrum the thermodynamic and kinetic quantities have power-law temperature dependence.

The most-detailed information on the order parameter can be obtained from phase-sensitive pairing symmetry tests.

These are based on Josephson tunneling and flux quantization: SQUID interferometry, tricrystal and tetracrystal magnetometry, magnetic flux imaging, and thin-film SQUID magnetometry (for review see Ref. 19 and references therein).

3. JOSEPHSON EFFECT AND SPONTANEOUS CURRENTS IN JUNCTIONS BETWEEN UNCONVENTIONAL SUPERCONDUCTORS

3.1. Superconducting weak links

The Josephson effect[8] arises in superconducting weak links—the junctions of two weakly coupled superconductors (massive banks) S_1 and S_2. The coupling (contacting) allows the exchange of electrons between the banks and establishes the superconducting phase coherence in the system as a whole. The weakness of the coupling means that the superconducting order parameters of the banks are essentially the same as for separate superconductors, and they are characterized by the phases of the order parameters χ_1 and χ_2. The Josephson weak link could be considered as the "mixer" of two superconducting macroscopic quantum states in the banks. The result of the mixing is a phase-dependent current-carrying state with current flowing from one bank to another. This current (Josephson current) is determined (parametrized) by the phase difference $\varphi = \chi_2 - \chi_1$ across the weak link.

Classification. General properties. According to the type of coupling, Josephson junctions can be classified as follows. 1) Tunnel junctions (originally considered by Josephson), S–I–S (I is an insulator layer). Weak coupling is provided by quantum tunneling of electrons through a potential barrier. 2) Junctions with direct conductivity, S–c–S (c is a geometrical constriction). These are the microbridges or point contacts. To have the Josephson behavior the constriction size must be smaller than the superconducting coherence length $\xi \sim \hbar v_F / \Delta$. 3) Junctions based on the proximity effect, S–N–S (N is a normal metal layer), S–F–S (F is a ferromagnetic metal layer). The different combinations of these types of junctions are possible, e.g., S–I–N–I–S or S–I–c–S structures. Another type of Josephson weak links are the multiterminal Josephson microstructures, in which the several banks (more than two) are coupled simultaneously with each other.[66–69]

An important characteristic of a Josephson junction is the current–phase relation (CPR) $I_s(\varphi)$. It relates the dc supercurrent flowing from one bank to another with the difference of the phases of the superconducting order parameter in the banks. The maximum value of $I_s(\varphi)$ determines the critical current I_c in the system. The specific form of the CPR depends on the type of weak link. Only in a few cases does it reduce to the simple form $I_s(\varphi) = I_c \sin(\varphi)$ that was predicted by Josephson for the case of a S–I–S tunnel junction. In the general case the CPR is a 2π-periodic function. For conventional superconductors it also satisfies the relation $I_s(\varphi) = -I_s(-\varphi)$. The latter property of CPR is violated in superconductors with broken time-reversal symmetry.[70–73] For general properties of the CPR and its form for different types of weak links the reader is referred to the books and reviews.[66,74–76]

Unconventional Josephson weak links. The properties of the current-carrying states in the weak link depend not only on the manner of coupling but also on the properties of the banks states. For example, the S–c–S junction with the banks subjected to external transport current was considered in Ref. 77. In such a system the time-reversal symmetry is artificially broken, which leads to some interesting features in the junction properties (the appearance of vortex-like states and a surface current flowing opposite to the tangential transport current in the banks). In this review we consider the junctions formed by unconventional (d-wave and triplet) superconducting banks, which we call unconventional Josephson weak links. The most striking manifestation of the unconventional symmetry of the order parameter in the junction is the appearance of a spontaneous phase difference and spontaneous surface current in the absence of current flowing from one bank to the other.

3.2. Junctions between *d*-wave superconductors

Measurements of the characteristics of unconventional Josephson weak links give information about the symmetry of superconducting pairing (see the review[78]). There are several approaches to the calculation of coherent current states in unconventional Josephson junctions. These include the Ginzburg–Landau treatment,[22] description in the language of Andreev bound states,[79] and the numerical solution of the Bogoljubov–de Gennes equations on a tight binding lattice.[80] A powerful method of describing inhomogeneous superconducting states is based on the quasiclassical Eilenberger equations for the Green's functions integrated over energy.[81] It was first used in Ref. 9 to describe the dc Josephson effect in a ballistic point contact between conventional superconductors. The Eilenberger equations can be generalized to the cases of d-wave and triplet pairing (Appendix II). In this Section we present the results of quasiclassical calculations for the Josephson and spontaneous currents in the grain boundary junction between d-wave superconductors.[12,16,17]

3.2.1. Current–phase relations

We consider a Josephson weak link $S_1^{(d)} - S_2^{(d)}$ which is formed by the mismatching of the orientations of the lattice axes in the banks $S_1^{(d)}$ and $S_2^{(d)}$, as shown in Fig. 4. The x axis is perpendicular and the y axis is parallel to the interface between two superconducting 2D half-spaces with different
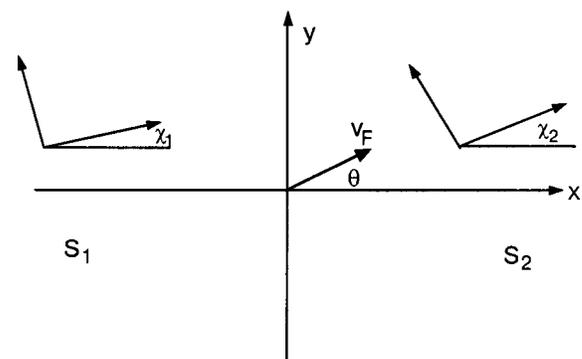

FIG. 4. Interface between two *d*-wave superconductors S_1 and S_2 with different orientations χ_1 and χ_2 of the lattice axes $a-b$.

$a-b$ axis orientations (angles χ_1 and χ_2 in Fig. 4). Far from the interface ($x \to \mp \infty$) the order parameter is equal to the bulk values $\Delta_{1,2}(\mathbf{v}_F)$. In the vicinity of the interface $x=0$, if the angles χ_1 and χ_2 do not coincide, the value of Δ deviates from $\Delta_{1,2}$. To describe the coherent current states in the system, the Eilenberger equations (A4) for the Green's functions must be solved simultaneously with the equation for Δ (A5). The equation of self-consistency (A5) determines the spatial distribution of $\Delta(\mathbf{r})$. The problem of solving the coupled equations (A4) and (A5) can be treated by numerical calculations. Analytical solutions can be obtained for the model (non-self-consistent) distribution of $\Delta(\mathbf{r})$:

$$\Delta(\mathbf{v}_F,\mathbf{r}) = \begin{cases} \Delta_1(\mathbf{v}_F)\exp(-i\varphi/2), & x<0, \\ \Delta_2(\mathbf{v}_F)\exp(i\varphi/2), & x>0. \end{cases} \quad (15)$$

The phase φ is the global phase difference between superconductors S_1 and S_2. In the following we consider the case of an ideal interface with transparency $D=1$. For the influence of interface roughness and effect of surface reflectancy ($D \neq 1$) as well as the numerical self-consistent treatment of the problem, see Ref. 16.

Analytical solutions in the model with the non-self-consistent order-parameter distribution (15) are presented in Appendix II. Using the expressions (A9), (A12) and (A13), we obtain the current densities $j_x(x=0) \equiv j_J$ and $j_y(x=0) \equiv j_S$:

$$j_J = 4\pi e N(0) v_F T \sum_{\omega>0} \left\langle \frac{\Delta_1 \Delta_2 |\cos\theta|}{\Omega_1 \Omega_2 + \omega^2 + \Delta_1 \Delta_2 \cos\varphi} \right\rangle \sin\varphi, \quad (16)$$

$$j_S = 4\pi e N(0) v_F T \sum_{\omega>0} \left\langle \frac{\Delta_1 \Delta_2 \sin\theta\,\mathrm{sign}(\cos\theta)}{\Omega_1 \Omega_2 + \omega^2 + \Delta_1 \Delta_2 \cos\varphi} \right\rangle \sin\varphi. \quad (17)$$

We denote by j_J the Josephson current flowing from S_1 to S_2 and by j_S the surface current flowing along the interface boundary. Expressions (16) and (17) are valid (within the applicability of the model (15)) for arbitrary symmetry of the order parameters $\Delta_{1,2}$. In particular, for s-wave superconductors from Eq. (16) we have the current–phase relation for the Josephson current in a conventional (s-wave) 2D ballistic S–c–S contact:[9]

$$j_J = 2 e N(0) v_F \Delta_0(T) \sin\frac{\varphi}{2} \tanh\frac{\Delta_0(T)\cos(\varphi/2)}{2T}.$$

The surface current j_S (17) equals zero in this case.

For a $S_1^{(d)} - S_2^{(d)}$ interface (DD junction) between d-wave superconductors, the functions $\Delta_{1,2}(\mathbf{v}_F)$ in (16) and (17) are $\Delta_{1,2} = \Delta_0(T)\cos 2(\theta - \chi_{1,2})$. In Appendix I the temperature dependence of the maximum gap $\Delta_0(T)$ in d-wave superconductors is presented for reference. The results of the calculations of $j_J(\varphi)$ and $j_S(\varphi)$ for a DD junction are displayed in Fig. 5 for different mismatch angles $\delta\chi$ between the crystalline axes across the grain boundary and at temperature $T = 0.1 T_c$ (assuming the same transition temperature on both sides). The interface is between two d-wave superconductors S_1 and S_2 with different $a-b$ lattice axis orientations χ_1 and χ_2.

In these figures, the left superconductor is assumed to be aligned with the boundary, while the orientation of the right
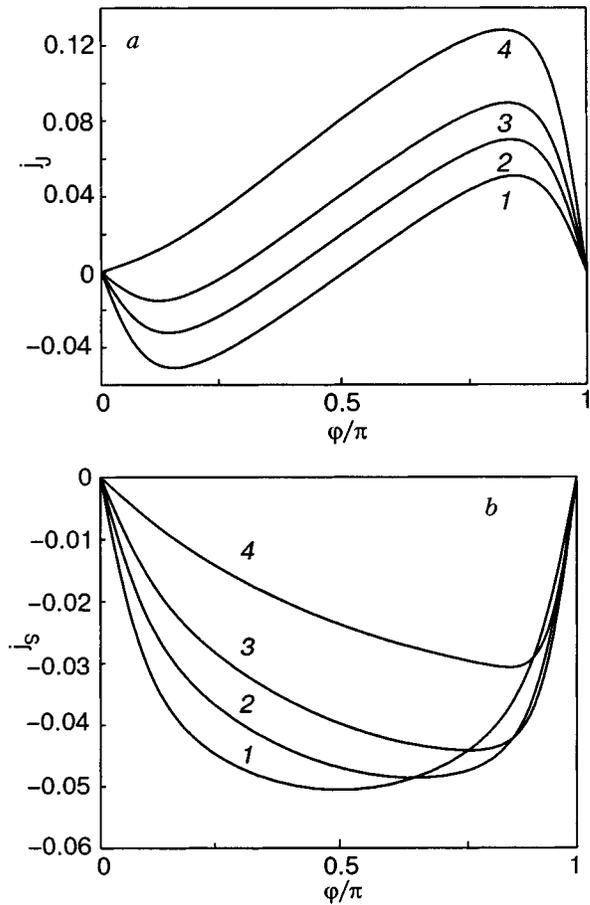

FIG. 5. Josephson current (a) and spontaneous current (b) versus the phase difference in a clean DD grain boundary junction calculated in a non-self-consistent approximation. Current densities are in units of $j_0 = 4\pi e N(0) v_F T$ and $T = 0.1 T_c$. The mismatch angles are $\chi_1 = 0$ and $\chi_2 = 45°$ (1), $40°$ (2), $34°$ (3), and $22.5°$ (4).

superconductor varies. The Josephson current–phase relation (Fig. 5a) demonstrates a continuous transition from a π-periodic (sawtooth-like) line shape at $\delta\chi = 45°$ to a 2π-periodic one for small $\delta\chi$, as expected in the case of a clean DND junction.[82] The phase dependence of the surface current (Fig. 5b) is also in qualitative agreement with results for SND and DND junctions.[83]

3.2.2. Spontaneous currents and bistable states

In contrast to the weak link between two conventional superconductors, the current j_S is not identically equal to zero. Moreover, in some region of angles χ_1 and χ_2 a value of the equilibrium phase difference $\varphi = \varphi_0$ exists at which $(dj_J(\varphi)/d\varphi)_{\varphi=\varphi_0} > 0$ and $j_J(\varphi_0) = 0$ but $j_S(\varphi_0) \neq 0$. These spontaneous phase difference φ_0 and spontaneous current $j_S(\varphi_0) \equiv j_{\mathrm{spon}}$ correspond to the appearance of time-reversal symmetry breaking states in the system (in fact, two values $\pm\varphi_0$ of the phase and corresponding spontaneous currents $\pm j_{\mathrm{spon}}$ appear). The region of $\mathcal{T}$-breaking states (as a function of temperature and mismatch angle) is shown in Fig. 6. In Figs. 6 and 7 we also present the self-consistent numerical result,[16] for comparison. Only in the asymmetric $\delta\chi = 45°$ junction does the degeneracy (at $\varphi = \pm\pi/2$) survive at all temperatures, due to its special symmetry which leads to complete suppression of all odd harmonics of $I(\varphi)$; gener-
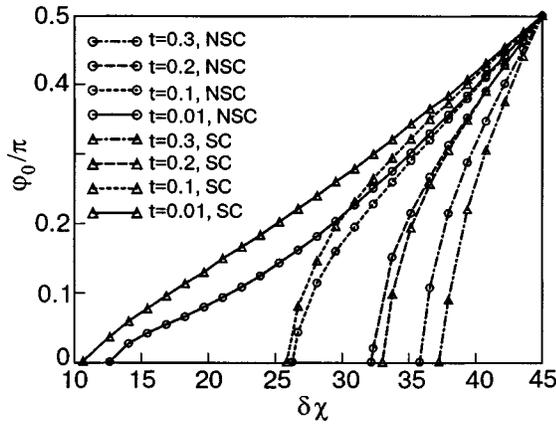
FIG. 6. Equilibrium phase difference in a clean DD grain boundary junction as a function of $\delta\chi = \chi_2 - \chi_1$ (keeping $\chi_1 = 0$), at different values of $t = T/T_c$. The circles and triangles correspond to non-self-consistent (NSC) and self-consistent (SC) calculations, respectively. For nonzero φ_0 the ground state is twofold degenerate ($\varphi = \pm\varphi_0$).

ally, $\varphi_0 \to 0$ at some temperature that depends on the orientation. The equilibrium value of the spontaneous current is nonzero in a certain region of angles and temperatures (Fig. 7), which is largest in the case of the asymmetric $\delta\chi = 45°$ junction.

The Josephson current $I_J(\varphi)$ is related to the Josephson energy of the weak link $E_J(\varphi)$ through $I_J(\varphi) = (2e/\hbar) \times (\partial E_J(\varphi)/d\varphi)$. The Josephson energy for DD junction as function of phase difference is shown schematically in Fig. 8. The arrows indicate two stable states of the system. These are two macroscopic quantum states which can be used for *d*-wave qubit design (see Sec. 4 below).

3.3. Junctions between triplet superconductors

The Josephson effects in the case of triplet pairing was first discovered[84,85] in weak links in ^{3}He. It was found that at low temperatures the mass current–phase dependence $J(\varphi)$ can essentially differ from the case of a conventional superconductor, and a so-called "π-state" ($J'(\pi) > 0$) is possible.[85,86] In several theoretical papers the Josephson effect has been considered for a pinhole in a thin wall separating two volumes of ^{3}He-*B*.[10,11,13,87–90] The discovery of metal superconducting compounds with triplet pairing of electrons has made topical the theoretical investigation of the Josephson effect in these superconductors. The Josephson effect is much more sensitive to dependence of $\Delta(\mathbf{k})$ on the
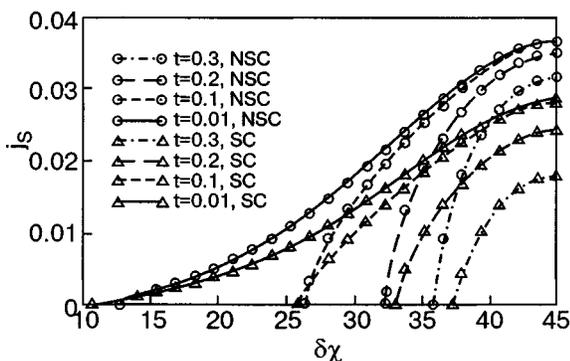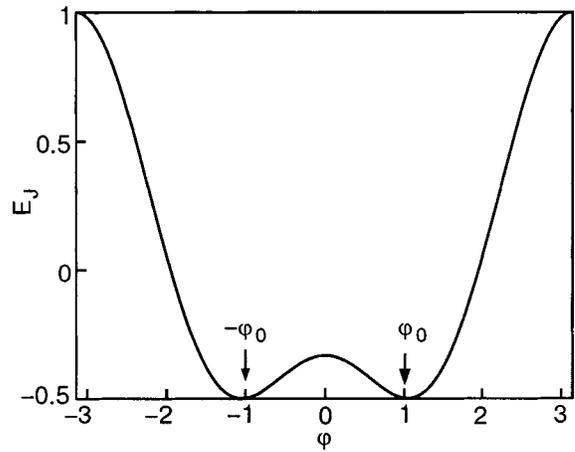

FIG. 8. Josephson energy of a DD junction.

momentum direction on the Fermi surface than are the thermodynamic and kinetic coefficients. In this Section the consideration of the Josephson effect in point contacts is based on the most favorable models of the order parameter in UPt$_3$ and Sr$_2$RuO$_4$, which were presented in Sec. 2.

3.3.1. Current density near an interface of misoriented triplet superconductors

Let us consider a model of the Josephson junction as a flat interface between two misoriented bulk triplet superconductors (Fig. 9). In this Section we follow the results of Ref. 15. In order to calculate the stationary Josephson current contact we use "transport-like" equations for ξ-integrated Green's functions[80] (see Appendix II.3). Here we consider the simple model of a constant order parameter up to the surface. The pair breaking and the electron scattering on the interface are ignored. For this non-self-consistent model the current–phase relation of a Josephson junction can be calculated analytically. This makes it possible to analyze the main features of the current–phase relations for different scenarios of "*f*-wave" superconductivity. We believe that under this strong assumption our results describe the real situation qualitatively, as was justified for point contacts between "*d*-wave" superconductors[12] and pinholes in ^{3}He.[91]

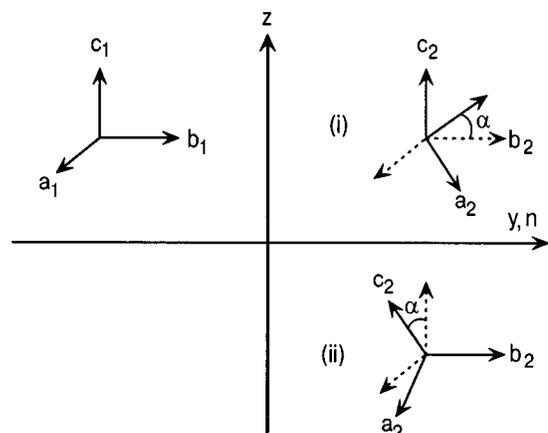FIG. 7. Spontaneous current in the junction of Fig. 6.

FIG. 9. Josephson junction as interface between two unconventional superconductors misorienated by an angle α and with order parameter $\mathbf{d}(\mathbf{k})$.

Knowing the component $\breve{g}_1(0)$ (A29) of the Green's function $\breve{g}(\hat{\mathbf{k}},\mathbf{r},\varepsilon_m)$, one can calculate the current density at the interface, $\mathbf{j}(0)$:

$$\mathbf{j}(0)=4\pi eN(0)v_F T\sum_{m=0}^{\infty} d\hat{\mathbf{k}}\hat{\mathbf{k}}\,\mathrm{Re}(\breve{g}_1(0)), \qquad (18)$$

where

$$\mathrm{Re}(\breve{g}_1(0))=\frac{\Delta_1\Delta_2}{2}\sum_{\pm}\frac{\sin(\pm\theta)}{_m^2+\Omega_1\Omega_2+\Delta_1\Delta_2\cos(\pm\theta)}. \qquad (19)$$

The real vectors $\Delta_{1,2}$ are related to the gap vectors $\mathbf{d}_{1,2}(\hat{\mathbf{k}})$ in the banks by the relation

$$\mathbf{d}_n(\hat{\mathbf{k}})=\Delta_n(\hat{\mathbf{k}})\exp(i\psi_n). \qquad (20)$$

The angle θ is defined by $\Delta_1(\hat{\mathbf{k}})\cdot\Delta_2(\hat{\mathbf{k}})=\Delta_1(\hat{\mathbf{k}})\Delta_2(\hat{\mathbf{k}})\cos\theta$, and $(\mathbf{k})=\psi_2(\hat{\mathbf{k}})-\psi_1(\hat{\mathbf{k}})+\varphi$.

Misorientation of the crystals would generally result in the appearance of a current along the interface,[17] as can be calculated by projecting the vector $\mathbf{j}$ on the corresponding direction.

We consider a rotation R in the right superconductor only (see Fig. 9), (i.e., $\mathbf{d}_2(\hat{\mathbf{k}})=R\mathbf{d}_1(R^{-1}\hat{\mathbf{k}})$). We choose the c axis in the left half-space along the partition between the superconductors (along the z axis in Fig. 9). To illustrate the results obtained by computing the formula (18), we plot the current–phase relation for different below-mentioned scenarios of "f-wave" superconductivity for two different geometries corresponding to different orientations of the crystals to the right and to the left at the interface (see Fig. 9): (i) The basal plane ab to the right is rotated about the c axis by the angle α; $\hat{\mathbf{c}}_1\|\hat{\mathbf{c}}_2$. (ii) The c axis to the right is rotated about the contact axis (y axis in Fig. 9) by the angle α; $\hat{\mathbf{b}}_1\|\hat{\mathbf{b}}_2$.

Further calculations require a definite model of the vector order parameter $\mathbf{d}$.

3.3.2. Current–phase relations and spontaneous surface currents for different scenarios of "f-wave" superconductivity

Let us consider the models of the order parameter in UPt$_3$ which are based on the odd-parity E_{2u} representation of the hexagonal point group D_{6h}. The first of them corresponds to the axial state (12) and assumes the strong spin–orbital coupling, with the vector $\mathbf{d}$ locked along the $\mathbf{c}$ axis of the lattice. The other candidate to describe the orbital states, which imply that the effective spin–orbital coupling in UPt$_3$ is weak, is the unitary planar state (13). The coordinate axes x,y,z here and below are chosen along the crystallographic axes $\hat{\mathbf{a}},\hat{\mathbf{b}},\hat{\mathbf{c}}$ as at the left in Fig. 9. These models describe the hexagonal analog of spin-triplet f-wave pairing.

In Fig. 10 we plot the Josephson current–phase relation $j_J(\varphi)=j_y(y=0)$ calculated from Eq. (18) for both the axial [with the order parameter given by Eq. (12)] and the planar [Eq. (13)] states for a particular value of α under the rotation of the basal plane ab to the right [the geometry (i)]. For simplicity we use a spherical model of the Fermi surface. For the axial state the current–phase relation is just a slanted sinusoid, and for the planar state it shows a "π-state." The
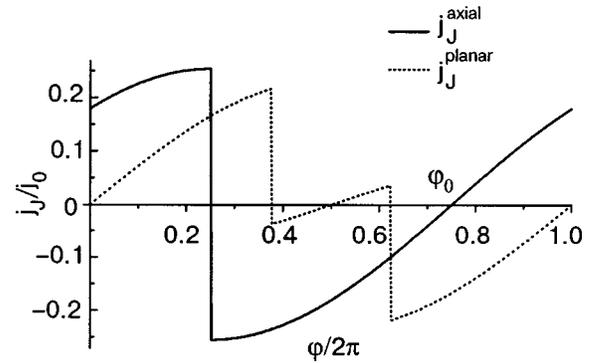

FIG. 10. Josephson current densities versus phase φ for axial (12) and planar (13) states in the geometry (i); misorientation angle $\alpha=\pi/4$; the current is given in units of $j_0=\pi/2\,eN(0)v_F\Delta_0(0)$.

appearance of the π-state at low temperatures is due to the fact that different quasiparticle trajectories contribute to the current with different effective phase differences $(\hat{\mathbf{k}})$ [see Eqs. (18) and (19)].[11] Such a different behavior can be a criterion for distinguishing between the axial and the planar states, taking advantage of the phase-sensitive Josephson effect. Note that for the axial model the Josephson current formally does not equal zero at $\varphi=0$. This state is unstable (does not correspond to a minimum of the Josephson energy), and the state with a spontaneous phase difference (value φ_0 in Fig. 10), which depends on the misorientation angle α, is realized.

The remarkable influence of the misorientation angle α on the current–phase relation is shown in Fig. 11 for the axial state in the geometry (ii). For some values of α (in Fig. 11 it is $\alpha=\pi/3$) there are more than one state which correspond to minima of the Josephson energy ($j_J=0$ and $dj_J/d\varphi>0$).

The calculated x and z components of the current, which are parallel to the surface, $\mathbf{j}_S(\varphi)$, are shown in Fig. 12 for the same axial state in the geometry (ii). Note that the current tangential to the surface as a function of φ is nonzero when the Josephson current (Fig. 11) is zero. This spontaneous tangential current is due to the specific "proximity effect," similar to spontaneous current in contacts between "d-wave" superconductors.[17] The total current is determined by the Green's function, which depends on the order parameters in both superconductors. As a result, for nonzero misorientation
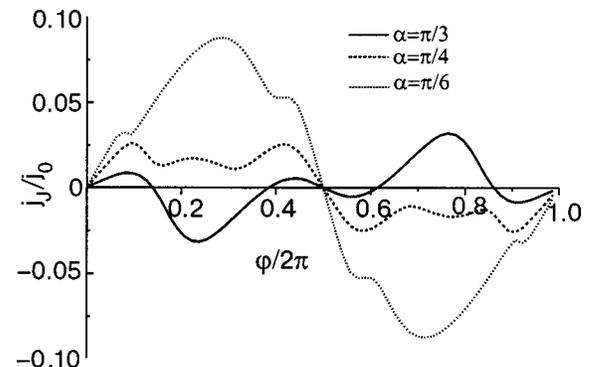

FIG. 11. Josephson current versus phase φ for the axial state (12) in the geometry (ii) for different α.
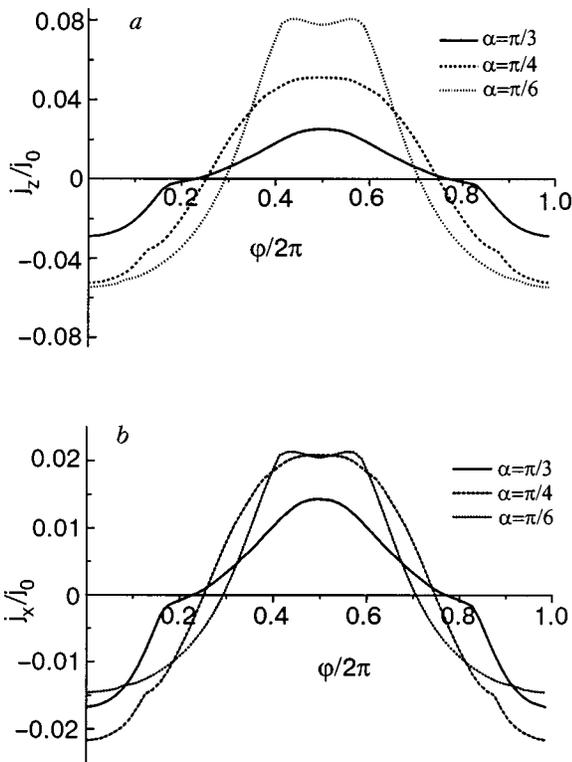
FIG. 12. z component (a) and x component (b) of the tangential current versus phase φ for the axial state (12) in the geometry (ii) for different α.

FIG. 14. Josephson current versus phase φ for the hybrid "f-wave" state (9) in the geometry (i) for different α.

angles a current parallel to the surface can be generated. In the geometry (i) the tangential current for both the axial and planar states at $T=0$ is absent.

The candidates for the superconducting state in Sr_2RuO_4 are the "p-wave" model (8) and the "f-wave" hybrid model (10). Taking into account the quasi-two-dimensional electron energy spectrum in Sr_2RuO_4, we calculate the current (18) numerically using the model of a cylindrical Fermi surface. The Josephson current for the hybrid "f-wave" model of the order parameter (Eq. (10)) is compared to the p-wave model (Eq. (8)) in Fig. 13 (for $\alpha = \pi/4$). Note that the critical current for the "f-wave" model is several times smaller (for the same value of Δ_0) than for the "p-wave" model. This different character of the current–phase relation enables us to distinguish between the two states.

In Figs. 14 and 15 we present the Josephson current and the tangential current for the hybrid "f-wave" model for different misorientation angles α (for the "p-wave" model it
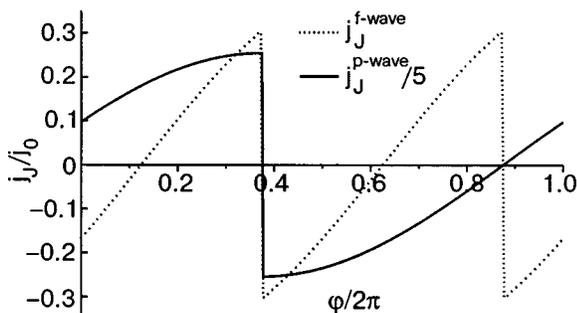
equals zero). Just as in Fig. 10 for the "f-wave" order parameter (12), in Fig. 14 for the hybrid "f-wave" model (9) the steady state of the junction with zero Josephson current corresponds to a nonzero spontaneous phase difference if the misorientation angle $\alpha \neq 0$.

Thus, in this Section the stationary Josephson effect in a planar junction between triplet superconductors is considered. The analysis is based on models with "f-wave" symmetry of the order parameter belonging to the two-dimensional representations of the crystallographic symmetry groups. It is shown that the current–phase relations are quite different for different models of the order parameter. Because the order parameter phase depends on the momentum direction on the Fermi surface, the misorientation of the superconductors leads to a spontaneous phase difference that corresponds to zero Josephson current and to the minimum of the weak-link energy. This phase difference depends on the misorientation angle and can possess any value. It has been found that in contrast to the "p-wave" model, in the "f-wave" models the spontaneous current may be generated in a direction which is tangential to the orifice plane. Generally speaking this current is not equal to zero in the absence of the Josephson current. It is demonstrated that the study of the current–phase relation of a small Josephson junction for different crystallographic orientations of banks enables one to judge the applicability of different models to the triplet superconductors UPt_3 and Sr_2RuO_4.

It is clear that such experiments require very clean superconductors and perfect structures of the junction because of pair-breaking effects of nonmagnetic impurities and defects in triplet superconductors.

4. JOSEPHSON PHASE QUBITS BASED ON d-WAVE SUPERCONDUCTORS

4.1. Quantum computing basics

As we have seen, unconventional superconductors support time-reversal symmetry breaking states on a macroscopic, or at least, mesoscopic scale. An interesting possibility arises then to apply them in quantum bits (*qubits*), basic units of quantum computers (see, e.g., Refs. 92–94), using $\mathcal{T}$-related states of the system as basic qubit states.

A quantum computer is essentially a set of N two-level quantum systems which, without loss of generality, can be represented by spin operators $\hat{\sigma}^{(i)}$, $i=1...N$. The Hilbert space of the system is spanned by 2^N states $|s_1\rangle \otimes |s_2\rangle \otimes \ldots$

FIG. 13. Josephson current versus phase φ for hybrid "f-wave" (10) and "p-wave" (8) states in the geometry (i); $\alpha = \pi/4$.
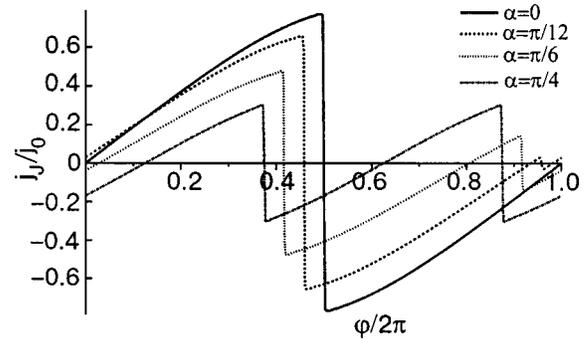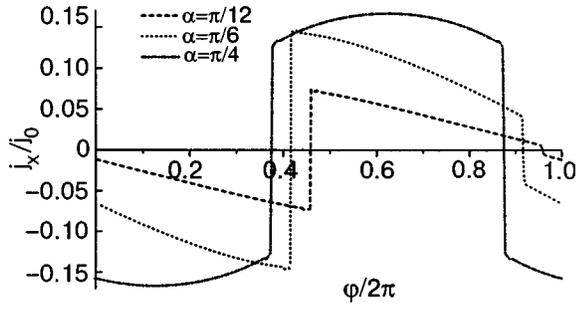
FIG. 15. Tangential current density versus phase φ for the hybrid "f-wave" state (9) in the geometry (i) for different α.

$\otimes |s_N\rangle$, $s_i = 0,1$. The information to be processed is contained in complex coefficients $\{\alpha\}$ of the expansion of a given state in this basis:

$$|\Psi\rangle = \sum_{s_j=0,1} \alpha_{s_1 s_2 \ldots s_N} |s_1\rangle \otimes |s_2\rangle \otimes \ldots \otimes |s_N\rangle. \qquad (21)$$

The unitary operations on states of the qubits are called gates, like in the classical case. Single qubit gates are $SU(2)$ rotations. An example of a two-qubit gate is a *conditional phase shift*, $CP(\gamma)$, which, being applied to a two-qubit wave function, shifts its phase by γ if and only if they are in the same ("up" or "down") state. In the basis $\{|0\rangle \otimes |0\rangle, |0\rangle \otimes |1\rangle, |1\rangle \otimes |0\rangle, |1\rangle \otimes |1\rangle\}$ it is

$$CP(\gamma) = \begin{pmatrix} e^{i\gamma} & 0 & 0 & 0 \\ 0 & 1 & 0 & 0 \\ 0 & 0 & 1 & 0 \\ 0 & 0 & 0 & e^{i\gamma} \end{pmatrix}. \qquad (22)$$

Obviously, if $CP(\gamma)$ is applied to a factorized state of two qubits, $|\Psi\rangle = (\alpha_1 |0\rangle + \beta_1 |1\rangle) \otimes (\alpha_2 |0\rangle + \beta_2 |1\rangle)$, in the general case we will obtain an *entangled* state. Up to an unimportant global phase factor, $CP(\gamma)$ results from the free evolution of two qubits, generated by the Hamiltonian $\mathcal{H} = J\hat{\sigma}_z^{(1)} \cdot \hat{\sigma}_z^{(2)}$, for a time $T = \hbar \gamma / (2J)$.

Another nontrivial example is the *controlled-not* gate CN_{12}, which, acting on $|s_1\rangle \otimes |s_2\rangle$, leaves s_1 intact and flips s_2 $(1 \to 0, 0 \to 1)$ if and only if $s_1 = 1$. The combination $SW_{12} = CN_{12}CN_{21}CN_{12}$ *swaps* (exchanges) the states of two qubits.

It can be shown that a universal quantum computer (that is, one that can realize any possible quantum algorithm, the way a Turing machine can realize any possible classical algorithm) can be modeled by a chain of qubits with only nearest-neighbor interactions:

$$\mathcal{H} = \sum_{i=1}^{N} \{u_i \sigma_z^{(i)} + \Delta_i \sigma_x^{(i)}\} + \sum_{i=j+1} J_{ij} \sigma_z^{(i)} \cdot \sigma_z^{(j)}. \qquad (23)$$

Further simplifications are possible,[95] but this would be irrelevant for our current discussion.

The operations of a quantum computer require that the parameters of the above Hamiltonian be controllable (more specifically, one must be able to *initialize, manipulate,* and *read out* qubits). For the unitary manipulations discussed above, at least some of the parameters u, Δ, J of the Hamiltonian must be controllable from the outside during the evo-

lution. Initialization and readout explicitly require nonunitary operations (projections). Therefore any practical implementation of a quantum computer must satisfy contradictory requirements: qubits must be isolated from the outside world to allow coherent quantum evolution (characterized by a decoherence time τ_d) for long enough time to allow an algorithm to run, but they must be sufficiently coupled to each other and to the outside world to permit initialization, control, and readout.[94] Fortunately, quantum error correction allows one to translate a larger size of the system into a longer effective decoherence time by coding each logical qubit in several logical ones (currently it is accepted that a system with τ_d / τ_g in excess of 10^4 can run indefinitely, where τ_g is the time of a single gate application (e.g., the time T in the example of $CP(\gamma)$).

Note that the operation of a quantum computer based on consecutive application of quantum gates as described above is not the only possible, or necessarily the most efficient, way of its use. In particular, it requires a huge overhead for quantum error correction. Alternative approaches have been suggested (e.g., adiabatic quantum computing[96–98]) which may be more appropriate for the smaller-scale quantum registers likely to be built in the immediate future.

4.2. Superconducting qubits

The size of the system is crucial not only from the point of view of quantum error correction. It is mathematically proven that a quantum computer is exponentially faster than a classical one in factorizing large integers; the number of known quantum algorithms is still small, but an active search for more potential applications is under way (see the above reviews and, e.g., Refs. 96–98). Nevertheless the scale on which its qualitative advantages over classical computers begin to be realized is about a thousand qubits. This indicates that solid-state devices should be looked at for the solution. The use of some microsopic degrees of freedom as qubits, e.g., nuclear spins of ^{31}P in a Si matrix, as suggested by Kane,[99] is attractive due to both the large τ_d and well-defined basis states. The difficulties in fabrication (due to small scale) and control and readout (due to weak coupling to the external controls) have not allowed realization of the scheme so far.

Among mesoscopic qubit candidates, superconducting, more specifically Josephson systems have the advantage of a coherent ground state and the absence or suppression of low-energy excitations, which increases the decoherence time. Together with well-understood physics and developed experimental and fabrication techniques, this makes them a natural choice.

The degree of freedom which is coupled to the control and readout circuits determines the physics of a qubit. In the superconducting case, one can then distinguish *charge* and *phase* qubits, depending on whether the charge (number of particles) or phase (Josephson current) of the superconductor is well defined.

The simplest example of a Josephson qubit is an rf SQUID,[100] with the Hamiltonian

$$\mathcal{H}_q = \frac{\hat{Q}^2}{2C} + \frac{\Phi_0^2}{8\pi^2 L}(\varphi - \varphi_x)^2 - \frac{I_c \Phi_0}{2\pi}\cos(\varphi), \qquad (24)$$

where L is the self-inductance of the loop, and I_c and C are the critical current and capacitance of the Josephson junction. The charge on the junction, $\hat{Q} = -2ie\partial_\varphi$, is conjugate to the phase difference φ across it. The external flux through the loop is $\Phi_x = \varphi_x \Phi_0/(2\pi)$. If it equals *exactly* $\Phi_0/2$ ($\varphi_x = \pi$) the $\mathcal{T}$-symmetry is broken. The potential part in (24) acquires a symmetric two-well structure, with tunneling between the wells possible due to the derivative term in (24), which reflects quantum phase uncertainty in a Josephson junction with finite capacitance. The tunneling rate is of the order of $\omega_p \exp(-U(0)/\omega_p)$, where the frequency of oscillations in one of the potential wells $\omega_p \sim \sqrt{E_J E_Q}$, and the height of the potential barrier between them $U(0) \sim E_J$.

The states in the right and left wells differ by the direction of the macroscopic persistent current and can be used as qubit states $|0\rangle$ and $|1\rangle$. The dynamics of the system is determined by the interplay of the charging energy $E_Q = 2e^2/C$ and Josephson energy $E_J = hI_c/(2e)$. Here $E_J/E_Q \gg 1$, and charging effects are responsible for the tunneling splitting of the levels. Coherent tunneling between them has actually been observed[100] in a Nb/AlO$_x$/Nb SQUID at 40 mK; the magnetic flux difference was approximately $\Phi_0/4$, which corresponded to currents of about 2 μA. (The actual design was a little more complicated than the simple rf SQUID.) Fine tuning of the external flux is essential to allow *resonant tunneling* through the potential barrier.

In the case of small loop inductance the phase will be fixed by flux quantization. For phase to tunnel, one has to introduce extra Josephson junctions in the loop. In the three-junction design,[101] two junctions are identical, each with a Josephson energy E_J, and the third one has a little smaller energy αE_J, $\alpha < 1$. In the presence of external flux φ_x, the energy of the system as a function of phases on the identical junctions φ_1, φ_2 is

$$\frac{U(\varphi_1, \varphi_2)}{E_J} = -\cos \varphi_1 - \cos \varphi_2 - \alpha \cos(\varphi_x + \varphi_1 - \varphi_2).$$

(25)

As before, if $\varphi_x = \pi$, the system has degenerate minima. Due to the two-dimensional potential landscape, tunneling between them does not require a large flux transfer of order $\Phi_0/2$, as in the previous case. Tunneling is again possible due to charging effects, which give the system an effective "mass" proportional to the Josephson junction capacitance C. Coherent tunneling between the minima has been observed.[102] The potential landscape (25) was recovered from measurements on a classical 3-junction loop (with C too large to allow tunneling).[103] Rabi oscillations were observed both indirectly, using the quantum noise spectroscopy[104] (the observed decay time of Rabi oscillation observed in these experiments $\tau_{\text{Rabi}} = 2.5$ μs), and directly, in time domain[105] ($\tau_{\text{Rabi}} = 150$ ns).

The above limit $E_J/E_Q \gg 1$ can be reversed. Then the design must include a mesoscopic island separated from the rest of the system by two tunnel junctions (a superconducting single electron transistor, SSET). The Hamiltonian becomes

$$\mathcal{H}_q = \frac{(\hat{Q} - Q_x)^2}{2C} - \frac{I_c \Phi_0}{2\pi} \cos \varphi,$$

(26)

where this time the role of external $\mathcal{T}$-symmetry breaking parameter is played by the charge Q_x induced on the island by a gate electrode. The working states are eigenstates of charge on the island; at appropriate Q_x the states with $Q = 2ne$ and $Q = 2(n+1)e$ are degenerate due to a parity effect,[106] where n is the number of Cooper pairs in the SSET. Quantum coherence in an SSET has been observed not just through the observation of level anticrossing near the degeneracy point, as in Refs. 100 and 102, but also in the time domain.[107] The system was prepared in a superposition of states $|n\rangle, |n+1\rangle$, kept at a degeneracy point for a controlled time τ, and measured. The probability $P(\tau)$ of finding the system in state n exhibited quantum beats.

A "hybrid" system, with $E_J/E_Q \simeq 1$, so-called "quantronium," was fabricated and measured in the time domain at CEA-Saclay,[108] with an extraordinary ratio $\tau_d/\tau_t \approx 8000$ (the tunneling time τ_t can be considered as the lower limit of the gate application time τ_g). Quantronium can be described as a charge qubit, which is read out through the phase variable, and is currently the best superconducting single qubit.

An interesting inversion of the quantronium design[109] is also a hybrid qubit, this time a flux qubit read out through the charge variable. It promises several advantages over other superconducting qubits, but has not yet been fabricated and tested.

Finally, a single current-biased Josephson junction can also be used as a qubit (phase qubit).[110,111] The role of basis states is played by the lowest and first excited states in the washboard potential. Rabi oscillations between them have been successfully observed.

The charge, hybrid, and phase qubits are mentioned here only for the sake of completeness, since unconventional superconductors are more naturally employed in flux qubits. Various Josephson qubits are reviewed in Ref. 112.

4.3. Application of *d*-wave superconductors to qubits

One of the main problems with the above flux qubit designs is the necessity of artificially breaking the $\mathcal{T}$-symmetry of the system by putting a flux $\Phi_0/2$ through it. Estimates show that the required accuracy is $10^{-5} - 10^{-6}$. The micron-size qubits must be positioned close enough to each other to make possible their coupling; the dispersion of their parameters means that applied fields must be locally calibrated; this is a formidable task given such sources of field fluctuations as fields generated by persistent currents in qubits themselves, which depend on the state of the qubit; field creep in the shielding; captured fluxes; magnetic impurities. Moreover, the circuitry which produces and tunes the bias fields is an additional source of decoherence in the system. (Similar problems arise in charge qubits, where the gate voltages must be accurately tuned.)

These problems are avoided if the qubit is *intrinsically bistable*. The most straightforward way to achieve this is to substitute the external flux by a static phase shifter, a Josephson junction with unconventional superconductors with non-zero equilibrium phase shift φ_0. From (25), one sees that, e.g., a three-junction qubit would require an extra π-junction ($\varphi_0 = \pi$).[113] In the same way a π-junction can be added to a multiterminal phase qubit.[114] The only difference compared to the case of external magnetic field bias is in the decoher-

ence time: instead of noise from field generating circuits we will have to take into account decoherence from nodal quasiparticles (see below).

A more interesting possibility is opened up if the bistable *d*-wave system is employed dynamically, that is, if its phase is allowed to tunnel between the degenerate values. In a so-called "quiet" qubit[113] an SDS′ junction (effectively two SD junctions in the (110) direction) is put in a low-inductance SQUID loop in parallel with a conventional Josephson junction and large capacitor. One of the SD junctions plays the role of a $\pi/2$-phase shifter. The other junction's capacitance C is small enough to make possible tunneling between $\pi/2$ and $-\pi/2$ states due to the charging term $Q^2/2C$. Two consecutive SD junctions are effectively a single junction with equilibrium phases 0 and π (which are chosen as working states of the qubit). The control mechanisms suggested in Ref. 113 are based on switches c and s. Switch c connects the small S′D junction to a large capacitor, thus suppressing the tunneling. Connecting s for the duration Δt creates an energy difference ΔE between $|0\rangle$ and $|1\rangle$, because in the latter case we have a frustrated SQUID with 0- and π-junctions, which generates a spontaneous flux $\Phi_0/2$. This is a generalization of applying the operation σ_z to the qubit. Finally, if switch c is open, the phase of the small junction can tunnel between 0 and π. Entanglement between qubits is realized by connecting them through another Josephson junction in a bigger SQUID loop. The suggested implementation for switches is based on a low-inductance dc-SQUID design with a conventional and a π-junction in parallel, with $I_{c,0} = I_{c,\pi}$. In the absence of external magnetic field the Josephson current through it is zero, while at external flux $\Phi_0/2$ it equals $2I_c$. Instead of external flux, another SDS′ junction, which can be switched by a voltage pulse between the 0 (closed) and π (open) states, is put in series with the π-junction.

The above design is very interesting. Due to the absence of currents through the loop during tunneling between $|0\rangle$ and $|1\rangle$ the authors called it "quiet," though, as we have seen, small currents and fluxes are still generated near the SD boundaries.

Another design based on the same bistability[115] only requires one SD or DD boundary. Here a small island contacts a massive superconductor, and the angle between the orientation of *d*-wave order parameter and the direction of the boundary can be arbitrary (as long as it is compatible with bistability). The advantage of such a design is that the potential barrier can to a certain extent be controlled and suppressed; moreover, in general there are two "working" minima $-\varphi_0, \varphi_0$; the phase of the bulk superconductor across the boundary is zero will be separated from each other by a smaller barrier than from the equivalent states differing by $2\pi n$. This allows us to disregard the "leakage" of the qubit state from the working space spanned by $(|0\rangle, |1\rangle)$, which cannot be done in a "quiet" design with exact π-periodicity of the potential profile. A convenient way of fabricating such qubits is to use grain-boundary DD junctions, where a two-well potential profile has indeed been observed.[104] Operations of such qubits are based on the tunable coupling of the islands to a large superconducting "bus"

and would allow the realization of a universal set of quantum gates.[116]

A more advanced design was fabricated and tested in the classical regime in Ref. 117. Here two bistable *d*-wave grain-boundary junctions with a small superconducting island between them are set in a SQUID loop. (The junctions themselves are also small, so that the total capacitance of the system allows phase tunneling.) In the case when the two junctions have the same symmetry but different critical currents, in the absence of external magnetic field there is no current passing through the big loop, and therefore the qubit is decoupled from the electromagnetic environment ("silent"). The second-order degeneracy of the potential profile at the minimum drastically reduces the decoherence due to coupling to the external circuits.

4.4. Decoherence in *d*-wave qubits

Decoherence is the major concern for any qubit implementation, especially for solid-state qubits, due to the abundance of low-energy degrees of freedom. In superconductors, this problem is mitigated by the exclusion of quasiparticle excitations due to the superconducting gap. This also explains why the very fact of existence of gapless excitations in high-T_c superconductors long served as a deterrent against serious search for macroscopic quantum coherence in these systems. An additional source of trouble may be zero-energy states (ZES) in DD junctions.

Nevertheless, recent theoretical analysis of DD junctions,[118,119] all using quasiclassical Eilenberger equations, shows that the detrimental role of nodal quasiparticles and ZES could be exaggerated.

Before turning to these results, let us first do a simple estimate of dissipation due to nodal quasiparticles in bulk *d*-wave superconductors.[120]

Consider, for example, a three-junction ("Delft") qubit with *d*-wave phase shifters. The $|0\rangle$ and $|1\rangle$ states support, respectively, clockwise and counterclockwise persistent currents around the loop, with superfluid velocity $\mathbf{v}_s$. Tunneling between these states leads to nonzero average $\langle \dot{\mathbf{v}}_s^2 \rangle$ in the bulk of the superconducting loop.

The time-dependent superfluid velocity produces a local electric field

$$\mathbf{E} = -\frac{1}{c}\dot{\mathbf{A}} = \frac{m}{e}\dot{\mathbf{v}}_s, \tag{27}$$

and quasiparticle current $\mathbf{j}_{qp} = \sigma\mathbf{E}$. The resulting average energy dissipation rate per unit volume is

$$\dot{\mathcal{E}} = \sigma E^2 \approx m\tau_{qp}\langle \bar{n}(v_s)\dot{v}_s^2 \rangle. \tag{28}$$

Here τ_{qp} is the quasiparticle lifetime, and

$$\bar{n}(v_s) = \int_0^\infty d\varepsilon\, \bar{N}(\varepsilon)[n_F(\varepsilon - p_F v_s) + n_F(\varepsilon + p_F v_s)] \tag{29}$$

is the effective quasiparticle density. The angle-averaged density of states inside the *d*-wave gap is[121]

$$\bar{N}(\varepsilon) \approx N(0)\frac{2\varepsilon}{\mu\Delta_0}, \tag{30}$$

where $\mu = \Delta_0^{-1} d|\Delta(\theta)|/d\theta$, and Δ_0 is the maximal value of the superconducting order parameter. Substituting (30) in (29), we obtain

$$\bar{n}(v_s) \approx N(0)\frac{2}{\mu\Delta_0}(-T^2)[\text{Li}_2(-\exp(-p_F v_s/T))$$
$$+ \text{Li}_2(-\exp(p_F v_s/T))], \qquad (31)$$

where $\text{Li}_2(z)$ is the dilogarithm. Expanding for small $p_F v_s \ll T$, we obtain

$$\bar{n}(v_s) \approx \frac{N(0)}{\mu\Delta_0}\left(\frac{\pi^2 T^2}{3} + (p_F v_s)^2\right). \qquad (32)$$

The two terms in parentheses correspond to thermal activation of quasiparticles and their generation by a current-carrying state. Note that a finite quasiparticle density by itself does not lead to any dissipation.

In the opposite limit ($T \ll p_F v_s$) only the second contribution remains,

$$\bar{n}(v_s) \approx \frac{N(0)}{\mu\Delta_0}(p_F v_s)^2. \qquad (33)$$

The energy dissipation rate gives the upper limit τ_ε for the decoherence time (since dissipation is a sufficient but not necessary condition for decoherence). Denoting by I_c the amplitude of the persistent current in the loop, by L the inductance of the loop, and by Ω the effective volume of the d-wave superconductor in which persistent current flows, we can write

$$\tau_\varepsilon^{-1} = \frac{2\dot{\mathcal{E}}\Omega}{LI_c^2} \approx \frac{2m\tau_{\text{qp}}N(0)\Omega\left(\frac{\pi^2 T^2}{3}\langle\dot{v}_s^2\rangle + p_F^2\langle v_s^2 \dot{v}_s^2\rangle\right)}{\mu\Delta_0 LI_c^2}. \qquad (34)$$

Note that the thermal contribution to τ_ε^{-1} is independent of the absolute value of the supercurrent in the loop ($\propto v_s$), while the other term scales as I_c^2. Both contributions are proportional to Ω and (via $\dot{v}_s$) to ω_t, the characteristic frequency of current oscillations (i.e., the tunneling rate between clockwise and counterclockwise current states).

It follows from the above analysis that the intrinsic decoherence in a d-wave superconductor due to nodal quasiparticles can be minimized by decreasing the amplitude of the supercurrent through it, and the volume of the material where *time-dependent* supercurrents flow.

Now let us estimate the dissipation in a DD junction. First, following Refs. 115 and 122, consider a DND model with ideally transmissive ND boundaries. Due to tunneling, the phase will fluctuate, creating a finite voltage on the junction, $V = (1/2e)\dot{\chi}$, and a normal current $I_n = GV$. The corresponding dissipative function and decay decrement are

$$\mathcal{F} = \frac{1}{2}\dot{\mathcal{E}} = \frac{1}{2}GV^2 = \frac{G\dot{\chi}^2}{2}\left(\frac{1}{2e}\right)^2; \qquad (35)$$

$$\gamma = \frac{2}{M_Q\dot{\chi}}\frac{\partial\mathcal{F}}{\partial\dot{\chi}} = \frac{G}{4e^2 M_Q} = \frac{4N_\perp E_Q}{\pi}. \qquad (36)$$

Here $E_Q = e^2/2C$, $M_Q = C/16e^2 = 1/32E_Q$, and $N_\perp$ are the Coulomb energy, effective "mass," and number of quantum channels in the junction, respectively. The last is related to

the critical Josephson current I_0 and spacing between Andreev levels in the normal part of the system, $\bar{\varepsilon} = v_F/2L$, via

$$I_0 = N_\perp e\bar{\varepsilon}. \qquad (37)$$

We require that $\gamma/\omega_0 \ll 1$, where $\omega_0 = \sqrt{32N_\perp E_Q\bar{\varepsilon}}/\pi$ is the frequency of small phase oscillations about a local minimum. This means that

$$N_\perp \ll \frac{\bar{\varepsilon}}{E_Q}. \qquad (38)$$

The above condition allows a straightforward physical interpretation. In the absence of thermal excitations, the only dissipation mechanism in the normal part of the system is through transitions between Andreev levels, induced by fluctuation voltage. These transitions become possible if $\bar{\varepsilon} < 2e\bar{V} \sim \sqrt{\bar{\chi}^2} \sim \omega_0$, which brings us back to (38). Another interpretation of this criterion arises if we rewrite it as $\omega_0^{-1} \gg (v_F/L)^{-1}$ (Ref. 115). On the right-hand side we see the time for a quasiparticle to traverse the normal part of the junction. If it exceeds the period of phase oscillations (on the left-hand side), Andreev levels simply do not have time to form. Since they provide the only mechanism for coherent transport through the system, the latter is impossible, unless our "no dissipation" criterion holds.

For a normal-layer thickness $L \sim 1000$ Å and $v_F \sim 10^7$ cm/s this criterion limits $\omega_0 < 10^{-12}$ s^{-1}, which is a comfortable two orders of magnitude above the tunneling splitting usually obtained in such qubits (~ 1 GHz) and can be accommodated in the above designs. Nevertheless, while presenting a useful qualitative picture, the DND model is not adequate for the task of extracting quantitative predictions.

A calculation[123] using the model of a DD junction interacting with a bosonic thermal bath gave an optimistic estimate for the quality of the tricrystal qubit, $Q > 10^8$.

The role of size quantization of quasiparticles in small DD and SND structures was suggested in Refs. 113 and 115. The importance of this effect is that it would exponentially suppress the quasiparticle density and therefore the dissipation below the temperature of the quantization gap, estimated as $1-10$ K. Recently this problem was investigated for a finite-width DD junction. Contrary to expectations, the size quantization as such turned out to be effectively absent on a scale exceeding ξ_0 (that is, practically irrelevant). From the practical point of view this is a moot point, since the decoherence time due to the quasiparticles in the junction, estimated in Ref. 119, already corresponds to a quality factor $\tau_\varphi/\tau_g \sim 10^6$, which exceeds by two orders of magnitude the theoretical threshold allowing a quantum computer to run indefinitely.

The expression for the decoherence time obtained in Ref. 119,

$$\tau_\varphi = \frac{4e}{\delta\varphi_2 I(\Delta t/e)}, \qquad (39)$$

where $\delta\varphi$ is the difference between equilibrium phases in degenerate minima of the junction (i.e., $\delta\varphi = 2\chi_0$ in other notation), contains the expression for the quasiparticle current in the junction at finite voltage, Δ_t/e (where Δ_t is the tunneling rate between the minima). This agrees with our back-of-the-envelope analysis: phase tunneling leads to finite

voltage in the system through the second Josephson relation, and with finite voltage comes quasiparticle current and decoherence. The quality factor is defined as $Q = \tau_\varphi \Delta_t / 2\hbar$, that is, we compare the decoherence time with the tunneling time. Strictly speaking, it is the quality factor with respect to the fastest quantum operation realized by the natural tunneling between the minima at the degeneracy point. For the Rabi transitions between the states of the qubit this number is much lower (10–20 versus 8000; Ref. 108) on account of the relatively low Rabi frequency.

A much bigger threat is posed by the contribution from zero-energy bound states, which can be at least two orders of magnitude larger. We can see this qualitatively from (39): a large density of quasiparticle states close to zero energy (i.e., at the Fermi level) means that even small voltages create large quasiparticle currents, which sit in the denominator of the expression for τ_φ. Fortunately, this contribution is suppressed in the case of ZES splitting, and such splitting is always present due, e.g., to the finite equilibrium phase difference across the junction.

A similar picture follows from the analysis presented in Ref. 124. A specific question addressed there is especially important: it is known that the RC constant measured in DD junctions is consistently 1 ps over a wide range of junction sizes,[125] and it is tempting to accept this value as the dissipation rate in the system. It would be a death knell for any quantum computing application of high-T_c structures, and nearly that for any hope to see some quantum effects there. Nevertheless, it is not quite that bad. Indeed, we saw that the ZES play a major role in dissipation in a DD junction but are sensitive to phase differences across it. Measurements of the RC constant are made in the resistive regime, when a finite voltage exists across the junction, so that the phase difference grows monotonically in time, forcing the ZES to approach the Fermi surface repeatedly. Therefore τ_{RC} reflects some averaged dissipation rate. On the other hand, in a free junction with not too high a tunneling rate the phase difference obviously tends to oscillate around χ_0 or $-\chi_0$, its equilibrium values, and does not spend much time near zero or π; therefore the ZES are usually shifted from the Fermi level, and their contribution to dissipation is suppressed.

This qualitative picture is confirmed by a detailed calculation. The decoherence time is related to the phase-dependent conductance via

$$\tau_\varphi = \frac{1}{\alpha F(\chi_0)^2 \delta E} \tanh \frac{\delta E}{2T}. \tag{40}$$

Here α is the dissipation coefficient, δE is the interlevel spacing in the well, and

$$G(\chi) = 4e^2 \alpha [\partial_\chi F(\chi)]^2. \tag{41}$$

For a realistic choice of parameters Eq. (40) gives a conservative estimate $\tau_\varphi = 1 - 100$ ns, and quality factor $Q \sim 1 - 100$. This is, of course, too little for quantum computing, but quite enough for observation of quantum tunneling and coherence in such junctions.

5. CONCLUSION

We have reviewed one of the most intriguing aspects of unconventional superconductivity, the generation of sponta-

neous currents in unconventional Josephson weak links. The mixing of the unconventional order parameters from the junction banks leads to the formation of a $\mathcal{T}$-breaking state in the weak link. A consequence of the time-reversal symmetry breaking is the appearance of a phase difference across the Josephson junction in the absence of current through the contact. This phenomenon, not present in conventional junctions between standard superconductors, radically changes the physics of weakly coupled superconductors. The current–phase relations for unconventional Josephson weak links, which we have discussed for $S^{(d)} - S^{(d)}$ and $S^{(\text{triplet})} - S^{(\text{triplet})}$ junctions, are quite different from the conventional one. Depending on the angle of misorientation of the d-wave order parameters in the banks, the current–phase relation $I_J(\varphi)$ is changed from a $\sin(\varphi)$-like curve to a $-\sin(2\varphi)$ dependence (Fig. 5). Clearly, it determines new features in the behavior of such a Josephson junction in applied voltage or magnetic field. We have discussed the simple case of an ideal interface between clean superconductors in which the spontaneous current generation effect is the most pronounced. Remaining beyond the scope of this review are a number of factors which complicate the simple models. They are the influence on the spontaneous current states of the interface roughness, potential barriers (dielectric layer), and scattering on impurities and defects in the banks. For the case of a diffusive junction see the article of Tanaka *et al.* in this issue. For the detailed theory of spontaneous currents in DD junctions see Ref. 16. The spatial distribution of spontaneous current, in particular, the effect of superscreening, is considered in Refs. 12 and 16. An important and interesting question concerns the possible induction of a subdominant order parameter near the junction interface and its influence on the value of spontaneous current. It was shown in Ref. 17 that the spontaneous currents decrease when there is interaction in the subdominant channel. This statement, which may seem paradoxical, can be explained in the language of current-carrying Andreev states (see Fig. 5 in Ref. 17). As a whole, the theory of unconventional Josephson weak links with breaking of $\mathcal{T}$ symmetry, in particular, the self-consistent consideration and nonstationary behavior, needs further development. The spontaneous bistable states in Josephson d-wave junctions attract considerable interest also from the standpoint of implementation of qubits, the basic units of quantum computers. In Sec. 4 we analyzed the application of d-wave superconductors to qubits. Unlike the Josephson charge and flux qubits based on conventional superconductors, the d-wave qubits have not yet been realized experimentally. Nevertheless, the important advantages of d-wave qubits, e.g., from the point of view of scalability, not to mention the fundamental significance of the $\mathcal{T}$-breaking phenomenon, demand future experimental investigations of unconventional weak links and devices based on them.

APPENDIX I. TEMPERATURE DEPENDENCE OF THE ORDER PARAMETER IN A *d*-WAVE SUPERCONDUCTOR

In a bulk homogeneous d-wave superconductor the BCS equation for the order parameter $\Delta(\mathbf{v}_F)$ takes the form
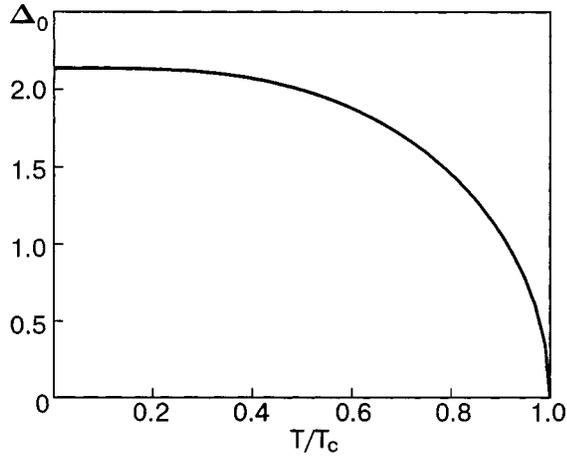
FIG. 16. Temperature dependence of the order parameter $\Delta_0(T)$ in a d-wave superconductor.

$$\Delta(\mathbf{v}_F) = 2\pi N(0)T \sum_{\omega > 0} \left\langle V(\mathbf{v}_F, \mathbf{v}'_F) \frac{\Delta(\mathbf{v}'_F)}{\sqrt{\omega^2 + |\Delta(\mathbf{v}'_F)|^2}} \right\rangle_{\mathbf{v}'_F} \tag{A1}$$

Or, writing $V(\mathbf{v}_F, \mathbf{v}'_F) = V_d \cos 2\theta \cos 2\theta'$, $\lambda_d = N(0)V_d$, $\Delta = \Delta_0(T)\cos 2\theta$, we have for $\Delta_0(T)$

$$\Delta_0(T) = \lambda_d 2\pi T \sum_{\omega > 0}^{\omega_c} \int_0^{2\pi} \frac{d\theta}{2\pi} \frac{\Delta_0(T)\cos^2 2\theta}{\sqrt{\omega^2 + \Delta_0(T)^2 \cos^2 2\theta}} \tag{A2}$$

($\omega = (2n+1)\pi T$, where ω_c is the cutoff frequency).

At zero temperature $T = 0$, in the weak coupling limit $\lambda_d \ll 1$, for $\Delta_0(T=0) = \Delta_0(0)$ it follows from (A2) that

$$\Delta_0(0) = 2\omega_c \beta \exp(-2/\lambda_d), \quad \ln \beta = \ln 2 - 1/2 \approx 1.21.$$

The critical temperature T_c is

$$T_c = \frac{2}{\pi}\omega_c \gamma \exp(-2/\lambda_d), \quad \ln \gamma = C = 0.577, \quad \gamma \approx 1.78.$$

Thus, $\Delta_0(0)/T_c = \pi\beta/\gamma \approx 2.14$.

In terms of T_c, Eq. (A2) can be presented in the form

$$\ln \frac{T}{T_c} = 2\pi T \sum_{\omega > 0}^{\infty} \left(2\int_0^{2\pi} \frac{d\theta}{2\pi} \frac{\cos^2 2\theta}{\sqrt{\omega^2 + \Delta_0(T)^2 \cos^2 2\theta}} - \frac{1}{\omega} \right). \tag{A3}$$

In the limiting cases, the solution of equation (A3) has the form

$$\Delta_0(T) = \begin{cases} \Delta_0(0)\left[1 - 3\varsigma(3)\left(\dfrac{T}{\Delta_0(0)}\right)^2\right], & T \ll T_c. \\[3mm] \left(\dfrac{32\pi^2}{21\varsigma(3)}\right)^{1/2} T_c\left(1 - \dfrac{T}{T_c}\right)^{1/2}, & T \sim T_c. \end{cases}$$

For arbitrary temperatures $0 \leqslant T \leqslant T_c$ the numerical solution of equation (A3) is shown in Fig. 16.

APPENDIX II. QUASICLASSICAL THEORY OF COHERENT CURRENT STATES IN MESOSCOPIC BALLISTIC JUNCTIONS

II.1. Basic equations

To describe the coherent current states in a superconducting ballistic microstructure we use the Eilenberger equations[80] for the ξ-integrated Green's functions

$$\mathbf{v}_F \cdot \frac{\partial}{\partial \mathbf{r}} \hat{G}_\omega(\mathbf{v}_F, \mathbf{r}) + [\omega\hat{\tau}_3 + \hat{\Delta}(\mathbf{v}_F, \mathbf{r}), \hat{G}_\omega(\mathbf{v}_F, \mathbf{r})] = 0, \tag{A4}$$

where

$$\hat{G}_\omega(\mathbf{v}_F, \mathbf{r}) = \begin{pmatrix} g_\omega & f_\omega \\ f_\omega^+ & -g_\omega \end{pmatrix}$$

is the matrix Green's function, which depends on the Matsubara frequency ω, the electron velocity on the Fermi surface $\mathbf{v}_F$, and the coordinate $\mathbf{r}$; here

$$\hat{\Delta} = \begin{pmatrix} 0 & \Delta \\ \Delta^+ & 0 \end{pmatrix}$$

is the superconducting order parameter. In the general case it depends on the direction of the vector $\mathbf{v}_F$ and is determined by the self-consistent equation

$$\Delta(\mathbf{v}_F, \mathbf{r}) = 2\pi N(0)T \sum_{\omega > 0} \langle V(\mathbf{v}_F, \mathbf{v}'_F) f_\omega(\mathbf{v}'_F, \mathbf{r}) \rangle_{\mathbf{v}'_F}. \tag{A5}$$

Solution of the matrix equation (A4) together with the self-consistent order parameter (A5) determines the current density $j(\mathbf{r})$ in the system:

$$\mathbf{j}(\mathbf{r}) = -4\pi ieN(0)T \sum_{\omega > 0} \langle \mathbf{v}_F g_\omega(\mathbf{v}_F, \mathbf{r}) \rangle_{\mathbf{v}_F}. \tag{A6}$$

In the following we will consider the two-dimensional case; $N(0) = m/2\pi$ is the 2D density of states and $\langle \ldots \rangle = \int_0^{2\pi} d\theta/2\pi \ldots$ is the averaging over directions of the 2D vector $\mathbf{v}_F$.

Supposing the symmetry $\Delta(-\mathbf{v}_F) = \Delta(\mathbf{v}_F)$, from the equation of motion (A4) and equation (A5) we have the following symmetry relations:

$$f^*(-\omega) = f^+(\omega); \quad g^*(-\omega) = -g(\omega);$$

$$f^*(\omega, -\mathbf{v}_F) = f^+(\omega, \mathbf{v}_F); \quad g^*(\omega, -\mathbf{v}_F) = g(\omega, \mathbf{v}_F);$$

$$f(-\omega, -\mathbf{v}_F) = f(\omega, \mathbf{v}_F); \quad g(-\omega, -\mathbf{v}_F) = -g(\omega, \mathbf{v}_F);$$

$$\Delta^+ = \Delta^*.$$

On the phenomenological level the different types of symmetry of the superconducting pairing are determined by the symmetry of the pairing interaction $V(\mathbf{v}_F, \mathbf{v}'_F)$ in Eq. (A5). For conventional (s-wave) pairing, the function $V(\mathbf{v}_F, \mathbf{v}'_F)$ is constant, V_s, and the corresponding BCS interaction constant is $\lambda = N(0)V_s$. In the case of d-wave pairing $V(\mathbf{v}_F, \mathbf{v}'_F) = V_d \cos 2\theta \cos 2\theta'$, $\lambda_d = N(0)V_d$. The angles θ and θ' determine the directions of vectors $\mathbf{v}_F$ and $\mathbf{v}'_F$ in the a–b plane.

II.2. Analytical solutions of Eilenberger equations in the model with non-self-consistent order parameter distribution

The solutions of equation (A5) for the Green's function $\hat{G}_\omega(v_f,\mathbf{r})$ can be easily obtained for model distribution (15) of $\Delta(\mathbf{r})$. For $x \leq 0$:

$$f(x,\theta) = \frac{\Delta_1 e^{-i\varphi/2}}{\Omega_1} + \frac{e^{-i\varphi/2}}{\Delta_1}(\eta\Omega_1 - \omega)e^{2x\Omega_1/|v_z|}C_1;$$
(A7)

$$f^+(x,\theta) = \frac{\Delta_1 e^{+i\varphi/2}}{\Omega_1} + \frac{e^{+i\varphi/2}}{\Delta_1}(-\eta\Omega_1 - \omega)e^{2x\Omega_1/|v_z|}C_1;$$
(A8)

$$g(x,\theta) = \frac{\omega}{\Omega_1} + e^{2x\Omega_1/v_z}C_1.$$
(A9)

For $x \geq 0$:

$$f(x,\theta) = \frac{\Delta_2 e^{+i\varphi/2}}{\Omega_2} + \frac{e^{+i\varphi/2}}{\Delta_2}(-\eta\Omega_2 - \omega)e^{-2x\Omega_2/|v_z|}C_2;$$
(A10)

$$f^+(x,\theta) = \frac{\Delta_2 e^{-i\varphi/2}}{\Omega_2} + \frac{e^{-i\varphi/2}}{\Delta_2}(\eta\Omega_2 - \omega)e^{-2x\Omega_2/|v_z|}C_2;$$
(A11)

$$g(z,\theta) = \frac{\omega}{\Omega_2} + e^{-2z\Omega_2/|v_z|}C_2.$$
(A12)

Matching the solutions at $x=0$, we obtain

$$C_1 = \frac{\Delta_1}{\Omega_1}\frac{\omega(\Delta_1 - \Delta_2\cos\varphi) + i\eta\Delta_2\Omega_1\sin\varphi}{(\Omega_1\Omega_2 + \omega^2 + \Delta_1\Delta_2\cos\varphi)},$$

$$C_2 = \frac{\Delta_2}{\Omega_2}\frac{\omega(\Delta_2 - \Delta_1\cos\varphi) + i\eta\Delta_1\Omega_2\sin\varphi}{(\Omega_1\Omega_2 + \omega^2 + \Delta_1\Delta_2\cos\varphi)}.$$
(A13)

Here $\Omega_{1,2} = \sqrt{\omega^2 + |\Delta_{1,2}|^2}$, $\eta = \text{sign}(v_x)$.

II.3. Quasiclassical Eilenberger equations for triplet superconductors

The "transport-like" equations for the ξ-integrated Green's functions $\check{g}(\hat{\mathbf{k}},\mathbf{r},\varepsilon_m)$ can be obtained for triplet superconductors:

$$[i\varepsilon_m\check{\tau}_3 - \check{\Delta}, \check{g}] + iv_F\hat{k}\nabla\check{g} = 0.$$
(A14)

The function $\check{g}$ satisfies the normalization condition

$$\check{g}\check{g} = -1.$$
(A15)

Here $\varepsilon_m = \pi T(2m+1)$ are discrete Matsubara energies, v_F is the Fermi velocity, and $\hat{\mathbf{k}}$ is a unit vector along the electron velocity, and $\check{\tau}_3 = \tau_3 \otimes \hat{I}$, and $\hat{\tau}_i$ $(i=1,2,3)$ are Pauli matrices in a particle–hole space.

The Matsubara propagator $\mathbf{g}$ can be written in the form:[96]

$$\check{g} = \begin{pmatrix} g_1 + \mathbf{g}_1\hat{\sigma} & (g_2 + \mathbf{g}_2\hat{\sigma})i\hat{\sigma} \\ i\hat{\sigma}_2(g_3 + \mathbf{g}_3\hat{\sigma}) & g_4 - \hat{\sigma}_2\mathbf{g}_4\hat{\sigma}\hat{\sigma}_2 \end{pmatrix},$$
(A16)

as can be done for an arbitrary Nambu matrix. The matrix structure of the off-diagonal self-energy Δ in Nambu space is

$$\check{\Delta} = \begin{pmatrix} 0 & i\mathbf{d}\hat{\sigma}\hat{\sigma}_2 \\ i\hat{\sigma}_2\mathbf{d}^*\hat{\sigma} & 0 \end{pmatrix}.$$
(A17)

Below we consider so-called unitary states, for which $\mathbf{d} \times \mathbf{d}^* = 0$.

The gap vector $\mathbf{d}$ has to be determined from the self-consistency equation:

$$\mathbf{d}(\hat{\mathbf{k}},\mathbf{r}) = \pi TN(0)\sum_m \langle V(\hat{\mathbf{k}},\hat{\mathbf{k}}')\mathbf{g}_2(\hat{\mathbf{k}}',\mathbf{r},\varepsilon_m)\rangle,$$
(A18)

where $V(\hat{\mathbf{k}},\hat{\mathbf{k}}')$ is the pairing interaction potential; $\langle...\rangle$ stands for averaging over directions of the electron momentum on the Fermi surface; $N(0)$ is the electron density of states.

Solutions of Eqs. (A14), (A18) must satisfy the conditions for the Greens's functions and the vector $\mathbf{d}$ in the banks of superconductors far from the orifice:

$$\check{g}(\mp\infty) = \frac{i\varepsilon_m\check{\tau}_3 - \check{\Delta}_{1,2}}{\sqrt{\varepsilon_m^2 + |\mathbf{d}_{1,2}|^2}};$$
(A19)

$$\mathbf{d}(\mp\infty) = \mathbf{d}_{1,2}(\hat{\mathbf{k}})\exp\left(\mp\frac{i\varphi}{2}\right),$$
(A20)

where φ is the external phase difference. Equations (A14) and (A18) have to be supplemented by the boundary continuity conditions at the contact plane and conditions of reflection at the interface between superconductors. Below we assume that this interface is smooth and the electron scattering is negligible. In a ballistic case the system of 16 equations for the functions g_i and $\mathbf{g}_i$ can be decomposed into independent blocks of equations. The set of equations which enables us to find the Green's function g_1 is

$$iv_F\hat{\mathbf{k}}\nabla g_1 + (\mathbf{g}_3\mathbf{d} - \mathbf{g}_2\mathbf{d}^*) = 0;$$
(A21)

$$iv_F\hat{\mathbf{k}}\nabla\mathbf{g}_- + 2i(\mathbf{d}\times\mathbf{g}_3 + \mathbf{d}^*\times\mathbf{g}_2) = 0;$$
(A22)

$$iv_F\hat{\mathbf{k}}\nabla\mathbf{g}_3 - 2i\varepsilon_m\mathbf{g}_3 - 2g_1\mathbf{d}^* - i\mathbf{d}^*\times\mathbf{g}_- = 0;$$
(A23)

$$iv_F\hat{\mathbf{k}}\nabla\mathbf{g}_2 + 2i\varepsilon_m\mathbf{g}_2 + 2g_1\mathbf{d} - i\mathbf{d}\times\mathbf{g}_- = 0,$$
(A24)

where $\mathbf{g}_- = \mathbf{g}_1 - \mathbf{g}_4$. For the non-self-consistent model ($\Delta_{1,2}$ does not depend on the coordinates up to the interface), Eqs. (A21)–(A24) can be solved by integrating over ballistic trajectories of electrons in the right and left half-spaces. The general solution satisfying the boundary conditions (A19) at infinity is

$$g_1^{(n)} = \frac{i\varepsilon_m}{\Omega_n} + iC_n\exp(-2s\Omega_n t);$$
(A25)

$$\mathbf{g}_-^{(n)} = \mathbf{C}_n\exp(-2s\Omega_n t);$$
(A26)

$$g_2^{(n)} = \frac{-2C_n\mathbf{d}_n - \mathbf{d}_n\times\mathbf{C}_n}{-2s\eta\Omega_n + 2\varepsilon_m}\exp(-2s\Omega_n t) - \frac{\mathbf{d}_n}{\Omega_n};$$
(A27)

$$g_3^{(n)} = \frac{2C_n\mathbf{d}_n^* + \mathbf{d}_n^*\times\mathbf{C}_n}{-2s\eta\Omega_n - 2\varepsilon_m}\exp(-2s\Omega_n t) - \frac{\mathbf{d}_n^*}{\Omega_n},$$
(A28)

where t is the time of flight along the trajectory, $\text{sign}(t) = \text{sign}(z) = s$; $\eta = \text{sign}(v_z)$; $\Omega_n = \sqrt{\varepsilon_m^2 + |\mathbf{d}_n|^2}$. By matching the solutions (A25)–(A28) at the orifice plane ($t=0$), we find the constants C_n and $\mathbf{C}_n$. The index n numbers the left

($n=1$) and right ($n=2$) half-spaces. The function $g_1(0)$ $=g_1^{(1)}(-0)=g_1^{(2)}(+0)$, which determines the current density in the contact, is

$$g_1(0) = \frac{i\varepsilon_m(\Omega_1+\Omega_2)\cos\varsigma + \eta(\varepsilon_m^2+\Omega_1\Omega_2)\sin\varsigma}{\Delta_1\Delta_2+(\varepsilon_m^2+\Omega_1\Omega_2)\cos\varsigma - i\varepsilon_m\eta(\Omega_1+\Omega_2)\sin\varsigma}. \tag{A29}$$

In formula (A29) we have taken into account that for unitary states the vectors $\mathbf{d}_{1,2}$ can be written as

$$\mathbf{d}_n = \Delta_n \exp i\psi_n, \tag{A30}$$

where $\Delta_{1,2}$ are real vectors.

*E-mail: kolesnichenko@ilt.kharkov.ua

[1] J. Bardeen, L. Cooper, and J. Schriffer, Phys. Rev. **108**, 1175 (1957).
[2] P. W. Anderson and P. Morel, Phys. Rev. **123**, 1911 (1961).
[3] R. Balian and N. R. Werthamer, Phys. Rev. **131**, 1553 (1963).
[4] A. J. Leggett, Rev. Mod. Phys. **47**, 331 (1975).
[5] D. Vollhardt and P. Wöfle, *The Superfluid Phases of* ³He, Taylor and Francis, New York (1990).
[6] G. Stewart, Rev. Mod. Phys. **56**, 755 (1984); G. Stewart, Z. Fisk, J. Willis, and J. L. Smith, Phys. Rev. Lett. **52**, 679 (1984).
[7] J. G. Bednorz and K. A. Muller, Z. Phys. B: Condens. Matter **64**, 189 (1986).
[8] B. D. Josephson, Phys. Lett. **1**, 251 (1962); B. D. Josephson, Adv. Phys. **14**, 419 (1965).
[9] I. O. Kulik and A. N. Omelyanchouk, Fiz. Nizk. Temp. **4**, 296 (1978) [Sov. J. Low Temp. Phys. **4**, 142 (1978)].
[10] J. Kurkijärvi, Phys. Rev. B **38**, 11184 (1988).
[11] S.-K. Yip, Phys. Rev. Lett. **83**, 3864 (1999).
[12] M. H. S. Amin, A. N. Omelyanchouk, and A. M. Zagoskin, in *New Trends in Superconductivity*, Kluwer, Dordrecht (2002), p. 95.
[13] M. Fogelstrom, S. Yip, and J. Kurkijärvi, Physica C **294**, 289 (1998).
[14] S. Yip, Phys. Rev. B **52**, 3087 (1995).
[15] R. Mahmoodi, S. N. Shevchenko, and Yu. A. Kolesnichenko, Fiz. Nizk. Temp. **28**, 262 (2002) [Low Temp. Phys. **28**, 184 (2002)].
[16] M. H. S. Amin, M. Coury, S. N. Rashkeev, A. N. Omelyanchouk, and A. M. Zagoskin, Physica B **318**, 162 (2002).
[17] M. H. S. Amin, A. N. Omelyanchouk, and A. M. Zagoskin, Phys. Rev. B **63**, 212502 (2001).
[18] V. P. Mineev and K. V. Samokhin, *Introduction to Unconventional Superconductivity*, Gordon and Breach, Amsterdam (1999).
[19] C. C. Tsuei and J. R. Kirtley, Rev. Mod. Phys. **72**, 969 (2000).
[20] J. Annett, N. Goldenfeld, and A. Leggett, *Physical Properties of High Temperature Superconductors*, Vol. 5, edited by D. M. Ginsberg, World Scientific, Singapore (1996).
[21] J. A. Sauls, Adv. Phys. **43**, 113 (1994).
[22] M. Sigrist, Prog. Theor. Phys. **99**, 899 (1998).
[23] R. Joynt and L. Taillefer, Rev. Mod. Phys. **74**, 235 (2002).
[24] L. D. Landau and E. M. Lifshitz, *Statistical Physics*, Part 1, Pergamon, New York (1979).
[25] M. Takigawa, P. C. Hammel, R. H. Heffer, and Z. Fisk, Phys. Rev. B **39**, 7371 (1989).
[26] V. Müller, Ch. Roth, E. W. Scheidt, K. Luders, E. Bucher, and N. E. Bommer, Phys. Rev. Lett. **58**, 1224 (1987).
[27] Y. J. Qian, M. F. Hu, A. Schedenstrom, H. P. Baum, J. B. Ketterson, D. Hinks, M. Levy, and B. K. Sarma, Solid State Commun. **63**, 599 (1987).
[28] Y. Maeno, H. Hashimoto, K. Yoshida, S. Nashizaki, T. Fujita, J. G. Bednorz, and F. Lichenberg, Nature (London) **372**, 532 (1994).
[29] Y. Maeno, Physica C **282−287**, 206 (1997).
[30] K. Kuroki, R. Arita, and H. Aoki, Phys. Rev. B **63**, 094509 (2001).
[31] H. Tou, Y. Kitaoka, K. Ishida, K. Asayama, N. Kimura, and Y. Onuki, Phys. Rev. Lett. **77**, 1374 (1996).
[32] K. Ishida, H. Mikuda, Y. Kitaoka, K. Asayama, Z. Q. Mao, Y. Mori, and Y. Maeno, Nature (London) **396**, 658 (1998).
[33] I. J. Lee *et al.*, cond-mat/0001332.
[34] K. Machida, T. Nishira, and T. Ohmi, J. Phys. Soc. Jpn. **68**, 3364 (1999).
[35] M. J. Graf, S.-K. Yip, and J. A. Sauls, Phys. Rev. B **62**, 14393 (2000).
[36] T. Dahm, H. Won, and K. Maki, preprint, cond-mat/0006301 (2000).
[37] M. J. Graf and A. V. Balatsky, Phys. Rev. B **62**, 9697 (2000).
[38] M. J. Graf, S.-K. Yip, and J. A. Sauls, J. Low Temp. Phys. **114**, 257 (1999).
[39] M. Sigrist, D. Agterberg, A. Furusaki, C. Honerkamp, K. K. Ng, T. M. Rice, and M. E. Zhitomirsky, Physica C **317−318**, 134 (1999).
[40] H. Won and K. Maki, Europhys. Lett. **52**, 427 (2000).
[41] Nishi Zaki *et al.*, J. Phys. Soc. Jpn. **69**, 572 (2000).
[42] I. Bonalde *et al.*, Phys. Rev. Lett. **85**, 4775 (2000).
[43] M. A. Tanatar *et al.*, Phys. Rev. B **63**, 64505 (2001).
[44] H. Matsui *et al.*, Phys. Rev. B **63**, 60505 (2001).
[45] Y. Maeno, T. M. Rice, and M. Sigrist, Phys. Today **54**, 42 (2001).
[46] T. M. Rice and M. Sigrist, J. Phys.: Condens. Matter **7**, L643 (1995).
[47] D. Agterberg, T. M. Rice, and M. Sigrist, Phys. Rev. Lett. **78**, 3374 (1997).
[48] L. Taillefer, B. Ellman, B. Lussier, and M. Poirier, Physica B **230**, 327 (1997).
[49] B. Lussier, B. Ellman, and L. Taillefer, Phys. Rev. B **53**, 5145 (1996).
[50] H. Suderow, J. P. Briston, A. Huxley, and J. Flouquet, J. Low Temp. Phys. **108**, 11 (1997).
[51] B. Ellman, L. Taillefer, and M. Porier, Phys. Rev. B **54**, 9043 (1996).
[52] G. E. Volovik and L. P. Gor'kov, Zh. Éksp. Teor. Fiz. **88**, 1412 (1985) [Sov. Phys. JETP **61**, 843 (1985)].
[53] A. Frusaki, M. Matsumoto, and M. Sigrist, Phys. Rev. B **64**, 054514 (2001).
[54] E. G. Volovik, JETP Lett. **55**, 368 (1992).
[55] E. G. Volovik, JETP Lett. **66**, 522 (1997).
[56] E. G. Volovik, and V. M. Yakovenko, J. Phys.: Condens. Matter **1**, 5263 (1980).
[57] V. M. Yakovenko, Phys. Rev. Lett. **65**, 251 (1990).
[58] V. M. Yakovenko, Phys. Rev. B **43**, 11353 (1991).
[59] E. G. Volovik and V. P. Mineev, Zh. Éksp. Teor. Fiz. **81**, 989 (1981) [Sov. Phys. JETP **54**, 524 (1981)].
[60] E. G. Volovik and V. P. Mineev, Zh. Éksp. Teor. Fiz. **86**, 1667 (1984) [Sov. Phys. JETP **59**, 972 (1984)].
[61] A. Furusaki, M. Matsumoto, and Manfred Sigrist, Phys. Rev. B **64**, 054514 (2001).
[62] A. I. Larkin, JETP Lett. **2**, 130 (1965).
[63] A. V. Balatsky *et al.*, Phys. Rev. B **51**, 15547 (1995).
[64] G. Preosti, H. Kim, and P. Muzikar, Phys. Rev. B **50**, 13638 (1994).
[65] G. A. Webb, *Nuclear Magnetic Resonance*, American Chemical Society (1997).
[66] K. K. Likharev, Rev. Mod. Phys. **51**, 101 (1979).
[67] I. O. Kulik, A. N. Omelyanchouk, and E. A. Kel'man, Fiz. Nizk. Temp. **3**, 1107 (1977) [Sov. J. Low Temp. Phys. **3**, 537 (1977)].
[68] R. de Bruyn Ouboter and A. N. Omelyanchouk, Superlattices Microstruct. **23**, 1005 (1999).
[69] M. H. S. Amin, A. N. Omelyanchouk, and A. M. Zagoskin, Fiz. Nizk. Temp. **27**, 835 (2001) [Low Temp. Phys. **27**, 616 (2002)].
[70] V. B. Geshkenbein, A. I. Larkin, and A. Barone, Phys. Rev. B **36**, 235 (1987).
[71] S. K. Yip, Phys. Rev. B **52**, 3087 (1995).
[72] Y. Tanaka and S. Kashiwaya, Phys. Rev. B **56**, 892 (1997).
[73] M. D. Fogelstrom, D. Rainer, and J. A. Sauls, Phys. Rev. Lett. **79**, 281 (1997).
[74] I. O. Kulik and I. K. Yanson, *The Josephson Effect in Superconductive Tunneling Structures*, Israel Program for Scientific Translation, Jerusalem (1972).
[75] A. Barone and G. Paterno, *Physics and Application of the Josephson Effect*, Wiley, New York (1982).
[76] A. A. Golubov, M. Yu. Kupriyanov, and E. Il'ichev, Rev. Mod. Phys. (2004) (in press).
[77] Yu. A. Kolesnichenko, A. N. Omelyanchouk, and S. N. Shevchenko, Phys. Rev. B **67**, 172504 (2004).
[78] R. Hlubina, M. Grajcar, and E. Il'ichev, cond-mat/0211255 (2002).
[79] T. Lofwander, V. S. Shumeiko, and G. Wendin, Phys. Rev. B **67**, R14653 (2000).
[80] Y. Tanuma, Y. Tanaka, M. Yamashiro, and S. Kashiwaya, Phys. Rev. B **57**, 7997 (1998).
[81] G. Eilenberger, Z. Phys. **214**, 195 (1968).
[82] A. M. Zagoskin, J. Phys.: Condens. Matter **9**, L419 (1997).
[83] A. Huck, A. van Otterlo, and M. Sigrist, Phys. Rev. B **56**, 14163 (1997).
[84] O. Avenet and E. Varoqaux, Phys. Rev. Lett. **60**, 416 (1988).
[85] S. Backhaus, S. Pereverzev, R. W. Simmond, A. Loshak, J. C. Davis, and R. E. Packard, Nature (London) **392**, 687 (1998).
[86] O. Avenet, Yu. Mukharsky, and E. Varoqaux, Physica B **280**, 130 (2000).
[87] E. V. Thuneberg, J. Kurkijärvi, and J. A. Sauls, Physica B **165&166**, 755 (1990).

[88]E. V. Thuneberg, M. Fogelström, and J. Kurkijärvi, Physica B **178**, 176 (1992).

[89]J. K. Vijas and E. V. Thuneberg, Phys. Rev. Lett. **83**, 3668 (1999).

[90]J. K. Vijas and E. V. Thuneberg, preprint, cond-mat/0107052 (2001).

[91]J. Viljas, preprint, cond-mat/0004246 (2000).

[92]A. Steane, Rep. Prog. Phys. **61**, 117 (1998).

[93]A. Kitaev, A. Shen', and M. Vialyj, *Classical and Quantum Calculations* [in Russian], Moscow MCNMO, CheRo (1999), p. 92.

[94]D. P. DiVincenzo, G. Burkard, D. Loss, and E. V. Sukhorukov, in *Quantum Mesoscopic Phenomena and Mesoscopic Devices in Microelectronics*, I. O. Kulik and R. Ellialtioglu (eds.), Vol. 559 of NATO Science Series C: Mathematical and Physical Sciences, Kluver (2000), p. 399.

[95]D. A. Lidar, L.-A. Wu, and A. Blais, Quant. Inf. Proc. **1**, 157 (2002).

[96]W. M. Kaminsky and S. Lloyd, quant-ph/0211152 (2002).

[97]E. Farhi, J. Goldstone, S. Gutmann, J. Lapan, A. Lundgren, and D. Preda, Science **292**, 472 (2001); quant-ph/0104129.

[98]W. Kaminsky, S. Lloyd, and T. P. Orlando, quant-ph/0403090.

[99]B. E. Kane, Nature (London) **393**, 133 (1999).

[100]J. R. Friedman, V. Patel, W. Chen, S. K. Tolpygo, and J. E. Lukens, Nature (London) **406**, 43 (2000).

[101]T. P. Orlando, J. E. Mooij, L. Tian, C. H. van der Wal, S. Levitov, S. Lloyd, and J. J. Mazo, Phys. Rev. B **60**, 15398 (1999).

[102]C. H. van der Wal, A. C. J. ter Haar, F. K. Wilhelm, R. N. Schouten, C. J. P. M. Harmans, T. P. Orlando, S. Lloyd, and J. E. Mooij, Science **290**, 773 (2000).

[103]E. Il'ichev, Th. Wagner, L. Fritzsch, J. Kunert, V. Schultze, T. May, H. E. Hoenig, H. G. Meyer, M. Grajcar, D. Born, W. Krech, M. V. Fistul, and A. M. Zagoskin, Appl. Phys. Lett. **80**, 4184 (2002).

[104]E. Il'ichev, N. Oukhanski, A. Izmalkov, Th. Wagner, M. Grajcar, H.-G. Meyer, A. Yu. Smirnov, A. Maassen van den Brink, M. H. S. Amin, and A. M. Zagoskin, Phys. Rev. Lett. **91**, 097906 (2003).

[105]I. Chiorescu, Y. Nakamura, C. J. P. M. Harmans, and J. E. Mooij, Science **299**, 1869 (2003).

[106]K. A. Matveev, M. Gisselfält, L. I. Glazman, M. Jonson, and R. I. Shekhter, Phys. Rev. Lett. **70**, 2940 (1993).

[107]Y. Nakamura, Yu. A. Pashkin, and J. S. Tsai, Nature (London) **398**, 786 (1999).

[108]D. Vion, A. Aassime, A. Cottet, P. Joyez, H. Pothier, C. Urbina, D. Esteve, and M. H. Devoret, Science **296**, 886 (2002).

[109]M. H. S. Amin, cond-mat/0311220.

[110]Y. Yu, S. Han, X. Chu, S.-I. Chu, and Z. Wang, Science **296**, 889 (2002).

[111]J. M. Martinis, S. Nam, and J. Aumentado, Phys. Rev. Lett. **89**, 117901 (2002).

[112]Y. G. Makhlin, G. Schoen, and A. Shnirman, Rev. Mod. Phys. **73**, 357 (2001).

[113]L. B. Ioffe, V. B. Geshkenbein, M. V. Feigel'man, A. L. Fauchere, and G. Blatter, Nature (London) **398**, 679 (1999).

[114]M. H. S. Amin, A. N. Omelyanchouk, A. Blais, A. Maassen van den Brink, G. Rose, T. Duty, and A. M. Zagoskin, Physica C **368**, 310 (2002).

[115]A. M. Zagoskin, cond-mat/9903170.

[116]A. Blais and A. M. Zagoskin, Phys. Rev. A **61**, 042308 (2000).

[117]M. H. S. Amin, A. Yu. Smirnov, A. M. Zagoskin, T. Lindstrom, S. Charlebois, T. Claeson, and A. Ya. Tzalenchuk, cond-mat/0310224.

[118]M. H. S. Amin, A. Yu. Smirnov, and A. Maassen van den Brink, Phys. Rev. B **67**, 100508(R) (2003).

[119]Ya. V. Fominov, A. A. Golubov, and M. Yu. Kupriyanov, cond-mat/0304383 (2003).

[120]A. M. Zagoskin, Doga: Turk. J. Phys. **27**, 491 (2003).

[121]D. Xu, D. K. Yip, and J. A. Sauls, Phys. Rev. B **51**, 16233 (1995).

[122]A. M. Zagoskin and M. Oshikawa, J. Phys.: Condens. Matter **10**, L105 (1998).

[123]D. M. Newns and C. C. Tsuei, US Patent No. US 6,495,854 B1 Dec. 17 (2002).

[124]M. H. S. Amin and A. Yu. Smirnov, Phys. Rev. Lett. **92**, 017001 (2004).

[125]A. Ya. Tzalenchuk, T. Lindstroöm, S. A. Charlebois, E. A. Sterantsov, Z. Ivanov, and A. M. Zagoskin, Phys. Rev. B **68**, 100501(R) (2003).